Optics and Lasers in Engineering 181 (2024) 108413

Contents lists available at ScienceDirect

Optics and Lasers in Engineering

journal homepage: www.elsevier.com/locate/optlaseng

Review

Application and development of optical-based viscosity measurement technology

Yan Ge [a,b], Xingxing Huang [a,b], Xusheng Tang [a,b], Yuntong Wang [a,b], Fuyuan Chen [a,b], Dongyang Xiao [c], Peng Liang [a,b,c,*], Bei Li [a,b,c,*]

[a] Changchun Institute of Optics, Fine Mechanics and Physics, Chinese Academy of Sciences, Changchun 130033, China
[b] University of Chinese Academy of Sciences, Beijing 100049, China
[c] Hooke Instruments Ltd., Changchun 130031, China

ARTICLE INFO

Keywords:
Viscosity
Optical technology
Low sample volumes
Non-contact measurement

ABSTRACT

Viscosity, as a crucial property of liquids, plays a vital role in various fields, including food, chemical, pharmaceutical, personal care, and biomedicine. Therefore, it is of great significance to develop methods that can accurately measure the viscosity of liquids in various environments. To this end, researchers have developed a variety of viscosity measurement techniques. In view of the complexity of viscosity measurement, viscosity measurement in many cases depends on optical technology. Optical-based viscosity measurement technology has demonstrated excellent performance at both macro and micro levels because of its suitability for low sample volumes and the advantages of non-contact measurement. Besides, it can be easily combined with other technologies and is suitable for a wide range of application scenarios. In this paper, we reclassify the optical technology used in the field of viscosity measurement, summarize the latest developments of optical technology in viscosity measurement, and discuss its future development direction. This review aims to assist researchers in mastering the latest developments in optical viscosity measurement techniques and to encourage experts in related fields to utilize and develop these techniques to address specific engineering requirements.

1. Introduction

Viscosity is a central parameter in describing fluid properties [1]. It not only determines the flow performance and energy loss of fluids but also plays a vital role in many industrial fields, including food processing [2-5], personal care [6,7], petrochemical [8], and biomedicine [9-12] etc. In the food industry, viscosity plays a significant role in determining the texture, taste, and stability of food products. For example, the increased viscosity of ice cream can enhance the richness of its taste and reduce the cold sensation for consumers. However, excessively high viscosity may also result in increased graininess, which can negatively impact the overall eating experience [13]. In the medical field, the viscosity of biological fluids such as blood [5] and plasma [14] is an important indicator for assessing health status. For some injectable biologic drugs, the viscosity shows an upward trend [15], but at the same time, too high viscosity levels may increase the difficulty of biologic drug preparation and the pain felt by the patient when administering the biologic drug [16-18]. Viscosity measurement encompasses a wide range of substances, from biodiesel [19,20] to polymers [21,22], from milk [23] to ice cream [24], from drugs [25,26] to cytoplasm [27,28], and mitochondria [29,30], spanning various fields and applications. Therefore, achieving accurate measurement of viscosity is a major research issue in many fields for various applications.

At present, there are many traditional viscometers used to measure fluid viscosity, including capillary viscometers, falling ball viscometers, rotational viscometers, and vibrating viscometers. The most common viscometer is the capillary viscometer [31], as shown in Fig. 1(a), which calculates viscosity by measuring the time it takes for the fluid sample in the upper sphere to flow through the capillary. It is low-cost but difficult to clean, easy to break, and has a long measurement time with low efficiency. The falling ball viscometer is shown in Fig. 1(b). The viscosity is calculated by recording the time of the upper and lower lines during the falling process, but the measurement accuracy is limited, which greatly limits its application range. A rotating viscometer, like the one shown in Fig. 1(c), is the most used viscometer, capable of measuring viscosity across a wide range of shear rates. However, its cost is high, and it may

* Corresponding authors.
E-mail addresses: liangpeng1@ciomp.ac.cn (P. Liang), beili@ciomp.ac.cn (B. Li).

https://doi.org/10.1016/j.optlaseng.2024.108413
Received 11 April 2024; Received in revised form 16 June 2024; Accepted 28 June 2024
Available online 19 July 2024

cause interfacial artifacts [32], which can affect the measurement accuracy. At small gap heights, plate misalignment can lead to additional secondary flows, affecting viscosity measurement accuracy [33]. Fig. 1 (d) depicts a vibration viscometer, which indirectly indicates the viscosity of a liquid by measuring the damping effect of solid vibration in the liquid. Its measurement accuracy is usually not as good as that of capillary viscometers and rotational viscometers. While the above viscometers basically enable viscosity measurements of samples, they require large sample volumes, which is not ideal for precious or limited samples.

To address the limitations of traditional viscosity measurement methods, scientists have proposed a variety of innovative viscosity measurement techniques, such as micro-electro-mechanical system (MEMS)-based viscometers. These techniques have attracted much attention due to their small size, high measurement accuracy, and capability to handle trace liquid [32,34,35]. However, many MEMS viscometers do not support non-contact measurement, such as Cantilever-based [36,37] and Diaphragm-based systems [38], whose tips need to be immersed in the solution to be measured. This immersion may introduce the risk of sample contamination. Nevertheless, these techniques still show great potential in the field of viscosity measurement [39].

In recent years, optical technology has developed a range of technologies and methods based on the understanding and use of light [40], such as optical imaging [41], optical tweezers [42], fiber optics [43], spectroscopy [44], etc. These technologies are widely used in manufacturing, communications, healthcare, and other fields. Optical techniques make use of physical properties (e.g., reflection, refraction, scattering, etc.) to detect and analyze the properties of a sample. These techniques typically do not necessitate direct contact with the sample, significantly reducing the need for sample volume. They achieve non-contact measurements with minimal sample volume, which not only shows the unique advantages of optical methods applied to the field of viscosity measurement, but also opens new paths for the development of viscosity measurement techniques.

The aim of this review is to provide an overview of the applications and new directions of optical techniques in the field of viscosity measurement, to help researchers to keep abreast of new advances in optical viscosity measurement techniques and to stimulate specialists in related fields to utilize and develop these techniques. Part I provides an overall assessment of the importance of viscosity measurement and discusses the advantages and disadvantages of various viscosity measurement methods. Part II provides an in-depth discussion of the fundamentals of optical techniques applied to viscosity measurement and provides specific application examples. Part III provides conclusions and perspectives on the measurement of viscosity by optical methods.

2. Optical methods for viscosity measurement

In this study, optical techniques for viscosity measurement are accurately classified, including Optical imaging Microfluidics, optical tweezers, light scattering technology, fiber optics, spectroscopy, and fluorescence. Optical imaging Microfluidics is regarded as a non-contact method for measuring viscosity at the macroscopic level due to its characteristics of measuring the whole sample. In contrast, light scattering technology, optical tweezers, fiber optics, spectroscopy, and fluorescence techniques focus on accurately measuring the local area of the sample, which are classified as local non-contact viscosity measurement techniques at the micro level. This classification method helps us better understand the unique functions and applicability of various optical techniques in viscosity measurement.

2.1. Optical imaging Microfluidics

Microfluidics, a technique for precisely manipulating fluid flow at the micron level, has had a profound impact on a wide range of disciplines, including chemical synthesis, bioanalysis, optics, and information technology [45]. In recent years, this technology has grown rapidly in recent years and is gradually transitioning from laboratory research to industrial production applications. Microfluidic chips, as the central component of this technology, can handle small sample volumes by utilizing their microscale channels. These chips are easy to handle, portable, and transparent [46], making it possible to integrate flow visualization and optical techniques to monitor the rheological properties of liquids in real time during the flow process [47].

Optical imaging Microfluidics is a combination of microfluidics and optical imaging technology. It utilizes equipment such as CCD and CMOS cameras, microscopes, laser confocal microscopes, and other tools to capture the movement of the liquid being measured within the microfluidic chip at the micro-nano scale. The viscosity of various liquids can be indirectly deduced through flow rate calculations, ratio calculations, and channel number analysis [46]. This paper categorizes the methods of measuring viscosity using optical microfluidics into unidirectional flow, co-flow, and droplet types based on the mechanism of manipulating liquids inside the microfluidic chip. These methods offer diverse measurement strategies for different application scenarios.

2.1.1. Measurement principles of viscosity by optical imaging Microfluidics

To deeply understand the basic principle of viscosity measurement by optical microfluidics, it is necessary to start with the fundamental concepts of viscosity, master the rheological properties of liquids, and understand their measurement mechanisms. This basic knowledge is crucial because it not only reveals the complexity of viscosity measurement but also clarifies why Optical imaging Microfluidics can be more effectively combined with viscosity measurement systems.

From the perspective of fluid dynamics, viscosity can be understood

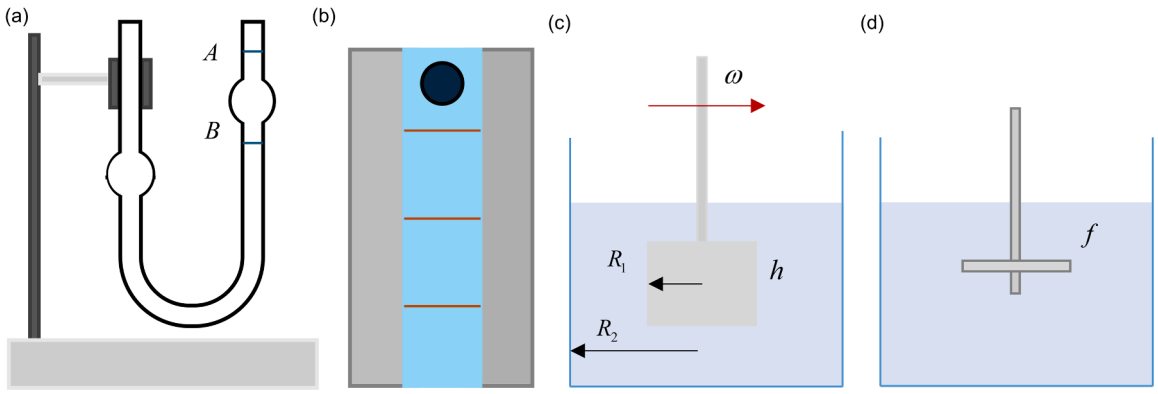

Fig. 1. (a) The capillary viscometer. (b) The falling ball viscometer. (c) The rotational viscometer. (d) The vibrating viscometer.

as the friction within a fluid, which gives the fluid the characteristic of resisting shape changes. According to the viscosity characteristics of the fluid, it can be classified into two main categories: Newtonian fluids and non-Newtonian fluids. The characteristic of Newtonian fluids is that their shear stress is proportional to the shear rate. This relationship can be expressed by the following formula:

$$\mu = \frac{\tau}{\gamma} \tag{1}$$

where μ is the dynamic viscosity coefficient of the fluid, $\tau$is the shear stress, and γ is the shear rate. Viscosity is the ratio of shear stress to shear rate. The dynamic viscosity of a fluid is only related to the temperature and pressure of the fluid, independent of external flow conditions [39]. However, in engineering practice, most fluids do not follow the simple linear relationship described above, which is called non-Newtonian fluid. The shear rate and shear stress can be expressed as follows:

$$\tau = \tau(\gamma) \tag{2}$$

The relationship between shear stress and shear rate of non-Newtonian fluids is more complex. It can be further classified into power-law fluids (such as shear-thinning fluids and shear-thickening fluids), Bingham fluids, viscoelastic fluids, and time-varying non-Newtonian fluids [48]. The relationship between shear stress and shear rate of Newtonian fluids and some non-Newtonian fluids can be expressed by Fig. 2, illustrating the complexity of dynamic viscosity measurement for non-Newtonian fluids. For applications that require offline measurement and limited sample volume, the microfluidic chip can serve as an ideal sample carrier. It can support microliters of liquid measurements, with transparency and ease of operation, making it very suitable for observation and analysis when combined with optical imaging techniques.

The principle of viscosity measurement is based on pushing the liquid through the microchannel under specific pressure conditions. When the liquid flow remains laminar in the microchannel and the fluid is assumed to be incompressible, the viscosity can be solved by Hagen-Poiseuille 's law.

$$\mu = \left(\mathrm{d}^2 / \mathrm{S}\right)\left(\Delta \mathrm{P} / \mathrm{vL}\right) \tag{3}$$

where vrepresents the average velocity, drepresents the depth of the pipe, L represents the distance that the liquid surface of the pipe advances at the corresponding time, ΔPrepresents the differential pressure inside the pipe, S is a constant specific to the channel geometry and μrepresents the liquid viscosity. This equation shows that viscosity is a physical quantity that can be determined directly when the differential pressure and liquid flow state are known. Optical imaging technology provides a non-contact detection method for observing the flow of liquid in microchannels. Thanks to the optical imaging technique, it is possible to capture the entire picture of the liquid flow inside the microchannel as long as the imaging field of view is large enough. This capability enables high-throughput viscosity measurement. In addition, the combination of optical methods and microfluidics allows us to efficiently measure the viscosity of non-Newtonian fluids.

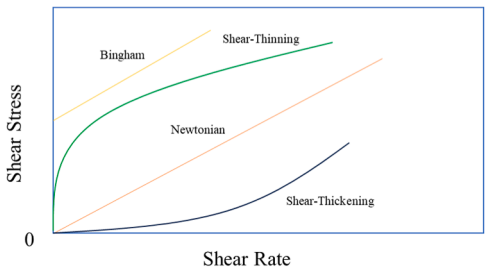

Fig. 2. The Relationship Between Shear Stress and Shear Rate of Newtonian and Non-Newtonian Fluids.

2.1.2. *Specific examples*

a) Unidirectional flow type

The working principle of the self-priming viscosity measurement device primarily relies on capillary force to drive the flow of the liquid. This process does not require the intervention of external power supply or moving parts. The operation method of this device is simple and has good repeatability. For a pipe with a rectangular cross-section, the capillary force can be described by the following formula:

$$\Delta \mathrm{P} = \mathrm{P}_{\mathrm{campillary}} = 2\sigma\cos\theta\left(\frac{1}{\mathrm{d}} + \frac{1}{\mathrm{w}}\right) \tag{4}$$

Where σ is the surface tension, θ is the contact angle, dand w are the height and depth of the cross-section, respectively. It can be seen from the formula that the capillary force is related to the surface tension of the liquid, the contact angle, and the geometry of the cross-section [49]. When measuring unknown fluids, such as biological fluids, these prior parameters are time-consuming and laborious to solve. Therefore, some researchers have proposed a self-calibrated microfluidic viscometer. Use other simple and invariant quantities instead of solving complex capillary forces. Srivastav et al. [49] utilized metal etching and photolithography to engrave nanoscale microchannels on a glass wafer. They employed optical adhesives to fabricate a nanoliter viscometer, which can be used to analyze blood and other solution samples. The microfluidic chip channels are divided into open and closed channels, as show in Fig. 3(a), which are used for measuring viscosity and solving capillary forces, respectively. A drop of liquid to be tested was placed at the entrance of the test channel. The liquid was sucked into the tube by capillary force, and the motion of the movement in the microfluidic channel was observed using an Olympus SZX12 stereomicroscope, and the viscosity of the liquid was calculated using the Hagen-Poiseuille equation. Afterwards, the serpentine-shaped closed pipe was modified into a closed gas chamber, as show in Fig. 3(b). By recording the change in the length of the liquid column inside the pipe, as show in Fig. 3(c), it was possible to generate different shear rates and obtain a better agreement with the non-Newtonian fluid viscosity values from the plate viscometer (AR 1000, TA Instruments) as show in Fig. 3(d), and to realize the non-Newtonian power law fluid viscosity. This microfabricated viscometer also enables the measurement of non-Newtonian power law fluids such as PEO and an ink-jet printing ink [50]. However, there are some limitations due to the relationship between shear rate and chip geometry, surface contact angle, etc., and the small range of shear rate variation. Meanwhile, this microfluidic chip fabrication method can only etch one chip at a time, which makes it difficult for mass production.

Later, Han et al. [51] fabricated a PDMS-based microfluidic viscometer using silicon molds and soft lithography. They pushed the liquid into the chip pipeline by dropping the liquid at the inlet and using capillary force and differential pressure. Subsequently, images were captured under a microscope by a CCD camera. Using deionized water as a reference liquid, the viscosity was calculated by comparing the flow distance and velocity between the sample liquid and the reference liquid, which required only 5μL or even less liquid. Morhell et al. [52] also verified the effectiveness of the viscometer by observing the changes in the liquid column inside a single-channel glass microfluidic chip using a USB microscope and also found that changes in the dynamic contact angle in the microchannels had a small effect on the fluid dynamics. Bamshad et al. [53] designed an integrated microfluidic viscometer using a micro-milling technique to fabricate rectangular microchannels on a PMMA sheet, which were then combined with another layer of PMMA sheet to form a closed fluid channel. Due to the surface tension between the fluid and the PMMA material and the capillary effect created by the shape of the microchannels, the fluid will automatically start to flow without the need for an external pump or

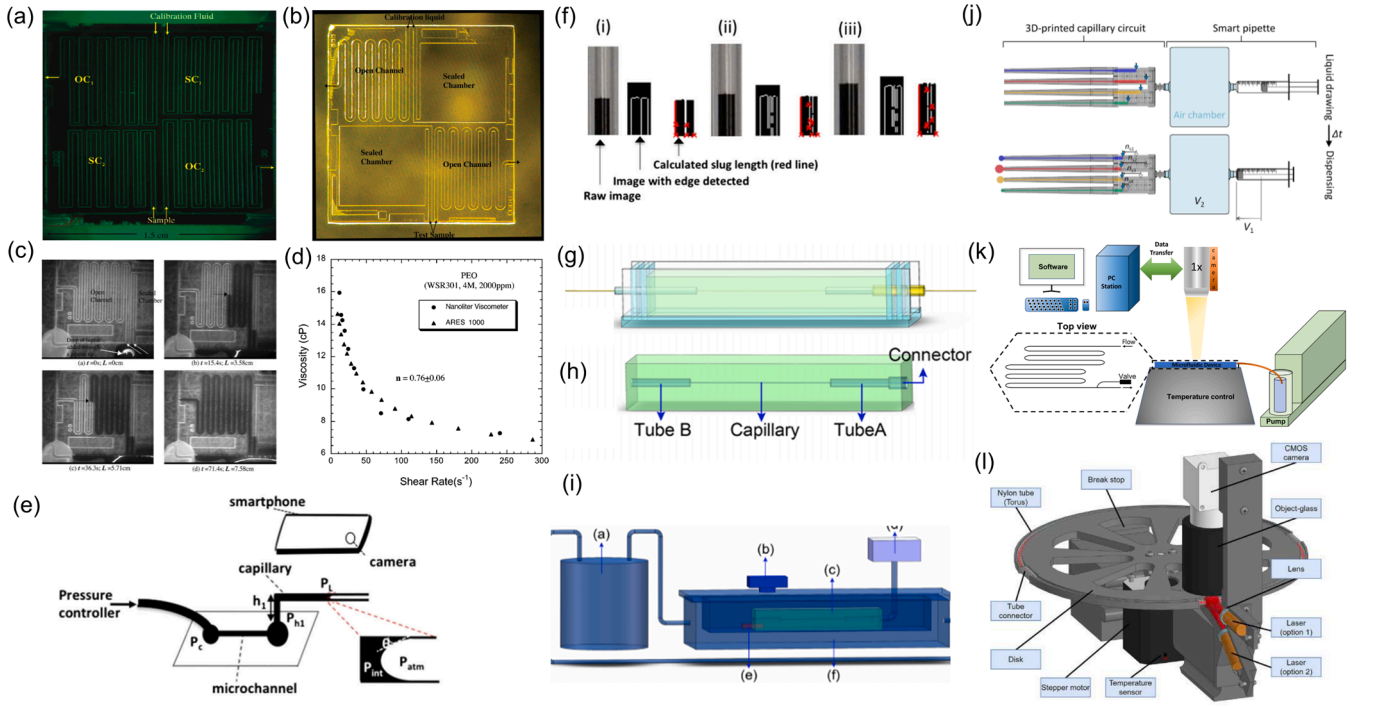

Fig. 3. (a) Self-calibrating nanoliter viscometer. (b) Self-calibrating microfabricated capillary viscometer. (c) Motion of the solution inside the viscometer. (d) Graph of the variation of PEO solution viscosity with shear rate as measured by the nanoliter viscometer and ARES 1000 at 23 °C. (e) Schematic diagram of the Capillary-based device. (f) Image processing step for calculating the distance travelled by a fluid flowing in a capillary over a period of time, showing a sequence of images at three different time points (i)-(iii), with each set of images consisting of the original video image, a processed image of the liquid column contour, and an image of the length of the liquid column identified using the Hough transform. (g) Schematic diagram of chip fabrication (h) Diagram of chip model. (i) Schematic diagram of the water bath heating device. (j) Schematic of the operation of the 3D printed capillary circuits (3D-CCs) viscometer. (k) Schematic of the microfluidic station. (l) Overview of the experimental setup: the 3d model.

other device to drive the flow. The microfluidic chip is combined with a photodetection system that uses a laser pointer and an electro-optical detection system to detect liquid flow and determine the dynamic viscosity of the liquid by measuring the time it takes for the liquid to flow between two specific points in the microchannel.

The range of shear rates that can be achieved by capillary-driven liquid flow is limited. To drive the liquid to be measured in a laminar motion within a pipe and achieve a wide range of shear rates, some have used an external pressure supply. The principle of slit shear rheology has been extensively utilized in numerous studies. When analyzing a power-law fluid within a rectangular slit pipe, the shear stress and shear rate can be solved by the following equation [54]:

$$\tau_w = \frac{\Delta pH}{2L} \tag{5}$$

$$\gamma = \left(\frac{2n+1}{3n}\right)\frac{6Q}{WH^2} = \frac{2n+1}{3n}\gamma_a \tag{6}$$

where L is the length, Δpis the pressure drop across the two segments of the rectangular cross-section pipe flow path, nis the exponent in the power law relationship, $\tau_w$is the shear stress, $\gamma$is the true shear rate, $\gamma_a$is the apparent shear rate, Q is the pipe flow rate, Wis the pipe width, and H is the pipe depth. Using optical imaging technology, we can calculate the flow velocity of the liquid. Combined with the cross-sectional size, we can know the flow rate and solve other parameters. With these parameters, the technician can efficiently calculate the shear viscosity of a fluid under specific conditions, thus providing an accurate method of analyzing the rheological properties of the fluid.

A pressure-driven Capillary-based shear microfluidic viscometer based on pressure drive was presented by Solomon et al. [55] Different driving pressures were applied to the system using an automated pressure controller using an automated pressure controller (MCFS-flex, Fluigent, France). By quantifying the pressure drop versus flow rate of a given fluid and incorporating slit rheology, the viscosity of the fluid is accurately determined. This Capillary-based viscometer uses PDMS material to create a slit-type pipe, backed up to a capillary tube, and a mobile phone lens to photograph the capillary fluid level advance at a given pressure, as show in Fig. 3(e). The velocity of the fluid as well as the flow rate is calculated by fitting a function of distance and time. Quantitative measurements of viscosity are achieved by means of flow rate, pressure, and cross-section size. The pressure-driven Capillary-based viscometer enables the measurement of viscosity over a wide range of shear rates, providing a reliable means of viscosity measurement for non-Newtonian fluids. This viscosity detection technique supports multi-channel parallel detection and multi-sample viscosity detection by capturing multiple capillaries on the image, and it also demonstrates the advantages of optical imaging for high-throughput viscosity measurement, and the experiments also involve image processing methods. As shown in Fig. 3(f), the images were processed according to the sequence of cropping image-applying threshold-edge detection-Hough transform. Verma et al. [56] found that thin nylon fibers can be embedded in PDMS, and easily removed after applying tension, and proposed a way of using nylon for processing 3D microchannels in PDMS, that avoids the complicated process of engraving a mold. Zou et al. [57] improved on this simple, clean, flexible, and low-cost microwire-molding microfabrication process by using fishing line, capillary, pp tube, and a special PMMA mold to construct a PDMS microfluidic chip as shown in Fig. 3(g). The capillary, reservoir, and pressure interface are all integrated into a single chip as in Fig. 3(h), which avoids the high-cost engraved mold. The viscosities of deionized water, a range of glycerol solutions, cell culture media, PBS and alcohols were measured experimentally using a digital camera, and the results were compared with those obtained by a conventional viscometer, enabling low-cost microfluidic viscosity measurement. A thermostatic

water bath such as Fig. 3 (i) was also provided to maintain a constant temperature to ensure accurate measurement of liquid viscosity at different temperatures.

Due to the high stability of the pressure peripheral to the gas source, the error of the gas source determines the upper limit of the viscosity measurement accuracy. To overcome this challenge, researchers have proposed a variety of novel viscosity measurement methods without a stable gas source. Oh and Choi [58] developed an innovative 3D printed capillary circuit (3D-CCs) technology for viscosity measurement. As shown in Fig. 3(j), the housing of the device is printed by stereo-lithography, while the capillary and fluid chambers are made of Tygon tubing pieces cut to a specific length [59] to ensure the accuracy of the measurement results. By using the modified syringe as a compressed gas chamber, the liquid to be tested is pushed through the capillary tube. By observing the scale lines in the fluid chamber, the researchers were able to analyze the viscosity characteristics of non-Newtonian fluids at different shear rates.

In addition to this, several new algorithms have been introduced into the field of viscosity measurement by optical imaging methods in recent years, and these algorithms have greatly enriched the techniques and methods of viscosity detection [60,61]. Giudice et al. [62] introduced machine learning into viscosity detection by using a high-speed digital microscope and camera to capture images of flowing particles, the experimental setup is shown in Fig. 3(k). Machine learning algorithms were used to automatically identify and track the particles in the video, which in turn calculated the shear viscosity and the longest relaxation time of the fluid. The introduction of machine learning enables fast and accurate processing of the video data, and the identification and tracking of particles in the microfluidic channel, which in turn makes the measurement of viscosity and the longest relaxation time faster and more reliable.

Deep Learning, as a branch of machine learning, is capable of automatically learning and extracting features from large amounts of data by constructing multi-layered neural network models that enable the recognition and prediction of complex patterns. The introduction of deep learning in viscosity detection means that key parameters, such as flow rate and shear rate, can be extracted directly from image data of fluid flow, and thus the viscosity of the fluid can be calculated. Recently, Kornaeva et al. [63] addressed the viscosity of whole blood, a non-Newtonian fluid with shear-thinning properties, by cleverly combining a capillary viscometer and a rotational viscometer, as shown in Fig. 3(l), where a high-speed CMOS camera was utilized to record the fluid flow images in the torus-shaped capillary viscometer, and the laser speckle-contrast imaging (LSCI) method was applied to capture the dynamic information of the fluid flow, which was subsequently processed and analyzed using pre-trained convolutional neural network (CNN) modules in deep learning, specifically the ResNet18 architecture, to predict the flow rates and shear rates. This not only improves the accuracy and efficiency of the measurements but also provides a new, automated approach to the analysis of fluid flow.

b) Co-flow

The method is based on the principle of laminar flow and uses a relative viscosity measurement method. Specifically, two co-flowing liquids are introduced simultaneously in a T-shaped channel structure at a certain flow rate: a reference liquid of known viscosity and an unknown liquid to be measured. These two liquids flow side-by-side in the channel, and the viscosity of the unknown liquid can be deduced by comparing the proportions of their positions at the interface within the channel. Optical imaging technology plays a central role in this process, providing a solid foundation for accurate measurements in co-flow viscometers.

Guillo et al. [64] used less than 300$\mu L$of fluid to calculate the average shear rate and its viscosity based on the physical properties of laminar parallel flow in a microfluidic T-channel using an optical microscope to determine the shape of the interface between the two fluids. Goel et al. [65] used a Leica Microscope to observe the "Y" type microfluidic chip to achieve viscosity measurements for biofuel blending. They used a syringe pump to pump glycerol and the bio-diesel blend to be measured at a constant flow rate, and observed that the less viscous fluids showed better mobility at the beginning of the flow, occupying a larger width in the straight pipe, and when the more viscous fluids entered the straight pipe they tended to occupy a wider pipe, and the viscosity of the unknown fluids could be determined by measuring the change of the width occupied by the fluids in the straight pipe, as in Fig. 4(a). This approach provides an effective technical solution for real-time monitoring of the blending and adulteration of biofuel. Venkateswaran et al. [66] used a small commercial microscope instead of the optical microscope used by Goel et al. to simplify the procedure and reduce the cost. They successfully solved the problem of milk adulteration using microfluidics. The microfluidic chip used was a "Y" shaped runner made of 3D transparent resin (MA-YG2005T) printed by stereo-lithography (SLA) technology, as shown in Fig. 4(b). By photographing the channel width occupied by the liquid to be tested at a specific runner position, effective detection of adulterated substances was achieved. Although this method depends on the viscosity of the reference liquid and can only detect the adulteration of a single substance, it enables the miniaturization and portability of the testing equipment. Hong et al. [67] used a microscope and a CMOS camera to observe a 3D-printed "T-type" channel microfluidic viscometer, which was used to detect the viscosity of glycerol mixtures. Kim et al. [68] further innovated by using a smartphone instead of a traditional camera to take pictures, and the experimental setup is shown in Fig. 4(c), where the sample and the reference fluid are delivered into the two inlets of a Y-shaped microfluidic device, and an interfacial line is induced at the downstream of the device. The interfacial width is measured by optical imaging to estimate the viscosity of the sample. With significant advantages in terms of fluidity, ease of operation, and data management, a hybrid system consisting of a smartphone and a microfluidic device can provide a mobile laboratory that performs a variety of testing and analysis functions related to healthcare.

Other researchers have designed microfluidic devices with multiple channels. Kang et al. [69] used a conventional polydimethylsiloxane (PDMS) replica molding technique to fabricate the microfluidic device. The device contained 100 indicator channels to measure the relative viscosity of the sample liquid. Fluorescent microfluidic patterns of SDS solution (Newtonian fluid) in the microfluidic channel array were photographed using an inverted epi-fluorescence microscope equipped with a cooled charge-coupled device (CCD) camera and the dynamic behavior of whole blood in the microfluidic channel array was captured using a high-speed CMOS camera. The initialized difference between the measured SDS solution (Newtonian fluid) and whole blood (non--Newtonian fluid) viscosities was less than 2.5 % and 2.0 %, respectively, when compared with a conventional viscometer. Subsequently, they developed a microfluidic viscometer with a fluid temperature controller. This device can accurately and simply measure Newtonian and non-Newtonian fluids without the need for a calibration procedure and can be a good solution to the problem of interface artefacts [70]. A CCD camera was used to take snapshots of the indicated number of channels filled by each fluid, and the number of channels occupied by the reference fluid was counted. On this basis, they [71] further improved the experimental equipment by designing a new microfluidic device. The device consists of two semicircular chambers, two side channels with multiple indication channels and a bridging channel. Also. Blood to be tested and a reference fluid of known viscosity (PBS solution) are introduced into the microfluidic chip. Blood was supplied from the femoral artery of the rat via a peristaltic pump, while the PBS solution was delivered via a syringe pump at a specific flow rate. Observations under stereo microscope were performed to indicate blood filling in the channels. Subsequently [72] utilized again to effectively monitor temporal changes in the biophysical properties of rat blood under ex vivo conditions, as shown in Fig. 4(d), further developed this technique by setting up an in-vitro system for closed loop, enabling the monitoring of

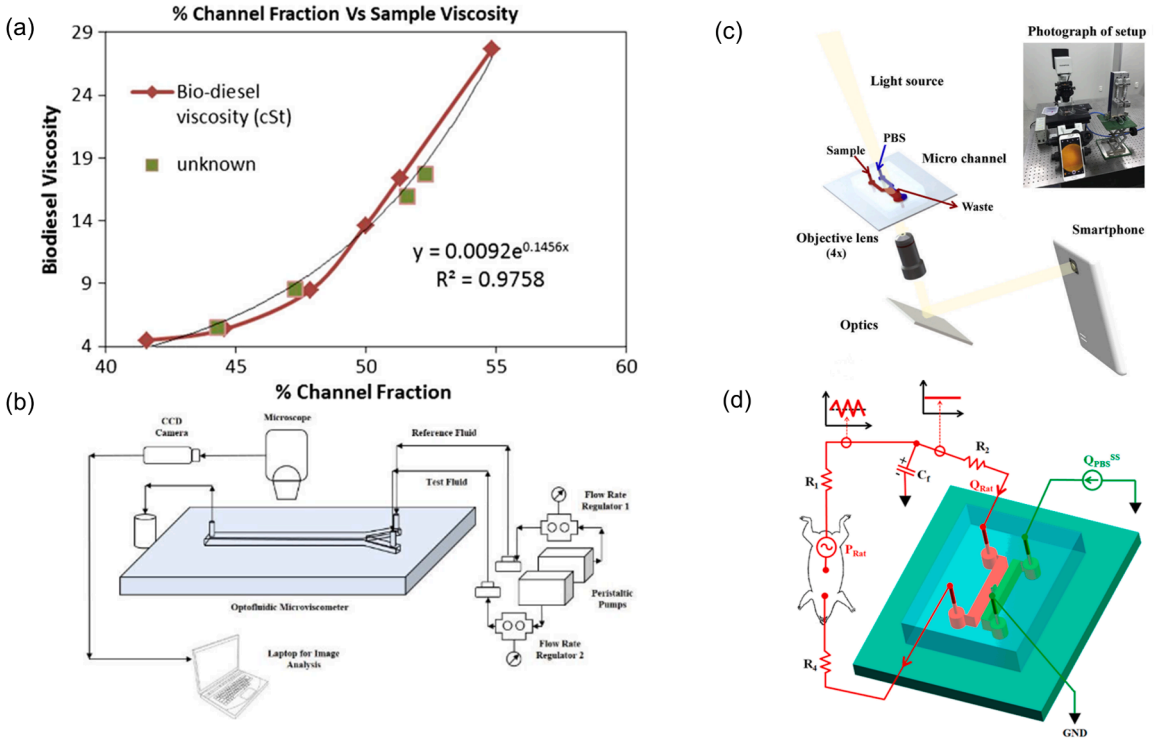

Fig. 4. (a) The schematic diagram of the relationship between channel fraction and viscosity. (b) Schematic of the Experimental Setup. (c) Schematics of experimental setup composed of smartphone, objective lens, and microfluidic device. (d) Schematics of the proposed working principle using three sequential flow controls in a microfluidic device for.

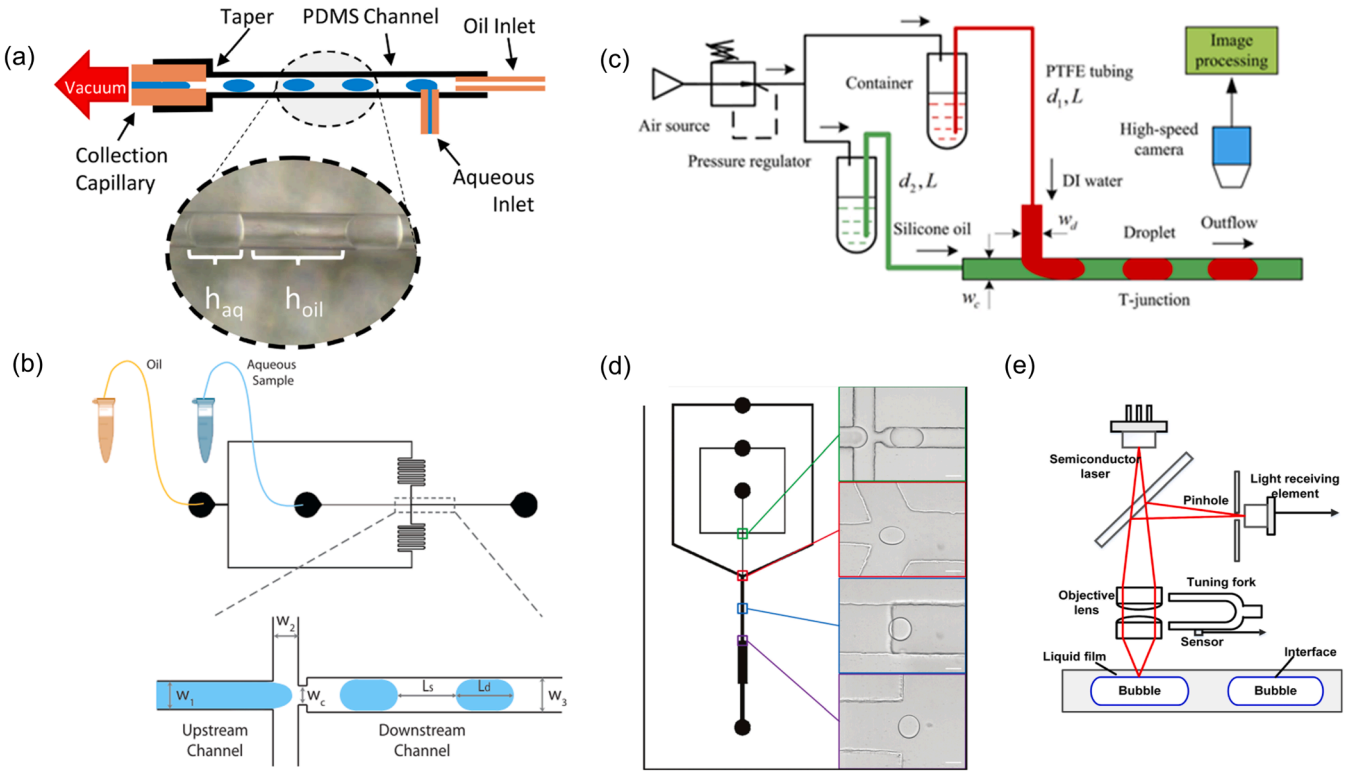

Fig. 5. (a) Height measurements of the aqueous and oil phases (h_{aq} and h_{oil}) from micrographs. (b) Schematic of the device layout and operation, with the oil phase in orange and the aqueous phase in blue, entering the device at a constant applied pressure. The length of the droplet in the downstream channel (L_d) is measured optically. (c) Schematic diagram of the device under pressure control. (d) Geometry of the microfluidic chip. (e) Principle of a laser confocal displacement meter.

temporal changes in blood viscosity and erythrocyte aggregation [73]. Solomon and Vanapalli [74] proposed a multiplexed viscometer, enabling high throughput viscosity measurement. Carnicer et al. [75] then utilized a high-resolution optical acquisition system to achieve very high shear rate measurement of the viscosity rheology of ceramic suspensions.

c) Droplet-based

Droplet microfluidics arises from the interaction of two immiscible fluids (e.g. oil and water) as they flow through a microchannel. In this process, the interface between the fluids is subjected to shear forces, resulting in the formation of droplets. The viscosity of the fluid affects the frequency and size of droplet generation, which provides a new idea for viscosity measurement [76].

Eric et al. [77] examined the viscosity of a glycerol-based sample of 101mpa.s using a nanoliter droplet viscometer with an average error of 6.6 % in the determination. The device uses a standard T-joint to generate aqueous-phase droplets in the oil phase. The sample droplets were driven through an abrupt contraction region by controlled pressure and a high-speed video camera was used to record the passage of the droplet interface through the contraction region, and the viscosity of the sample was calculated by observing the flow rate of the droplet interface through the region, and thus the viscosity of the sample was calculated. The mechanism of the formation of the T-structure droplets was investigated by a high-speed video camera and microscope by Wehking et al. [78] DeLaMarre et al. [79] reported a microfluidic capillary viscometer that can form droplets of aqueous samples in an unmixed carrier phase, and measure the dimensions of the resulting droplets using a stereoscopic dissection microscope and a microscope camera,as shown in Fig. 5(a), to encode information about the viscosity of the sample. The device has excellent calibration stability, with a calibration factor of only 0.6 % drift per run, and is capable of handling both aqueous and non-aqueous samples. Li et al. [80] developed a droplet-based water--in-oil continuous viscometer, as shown in Fig. 5(b), which is capable of measuring viscosity changes in 10 s or less and consumes a total sample volume of less than 1μLper hour. The viscometer uses a flow-focusing geometry that produces droplets at a constant pressure. Observations are recorded using an inverted microscope (Nikon Eclipse Ti) and a CCD camera. The device not only measures viscosity, but also allows for reactions and analyses in solutions with significant changes in viscosity. A thin oil layer between the sample and the channel wall protects the sample from cross-contamination, making the device compatible with biological applications as well. The range and sensitivity of the viscometer can be varied by changing the viscosity of the oil phase, i.e., the range of viscosity measurement is also held by the viscosity of the oil phase. In addition, they investigated a continuous viscometer for measuring blood coagulation, which uses pneumatic pressure to propel the oil phase and blood through a tube and observe the viscosity changes during blood coagulation at a constant shear rate [81]. Zeng et al. [82] used a T-connected microdroplet generator to produce a single dispersed droplet, and regulated flow rates of both the continuous and dispersed phases by a pressure-controlled microfluidic device. They used a high-speed camera with a maximum frame rate of up to 2000 fps to measure the length of the droplets in the microchannel and calculated the fluid viscosity of the continuous phase by analyzing the viscosity ratio of the two phases, as shown in Fig. 5(c).

André et al. [83] proposed an innovative approach to viscosity measurement methodology of determining the viscosity of the internal phase of a droplet by analyzing the shape of the droplet as it expands. This requires that the surface tension between the two liquids, the flow rate, the geometry of the channel and the viscosity of the continuous phase are known. They designed a PDMS microfluidic chip, as shown in Fig. 5(d), equipped with an inverted microscope, and used a high-speed camera to record droplet images. In the experiment, various parameters such as droplet radius, chamber height, geometrical parameters, droplet velocity and interfacial tension were varied. Therefore, multiple experiments with different parameter variations were conducted to ensure the rigor of the experiment. In addition, they measured the interfacial tension and considered the potential effect of surfactants. This research lays the foundation for high-throughput research in the field of digital microfluidics.

In addition to the use of oil-water two-phase dispersion into small droplets, some researchers have also generated gas-liquid two-phase by gas for viscosity measurement. Sun et al. [84] developed an on-line measurement technique for the determination of surface tension and viscosity of fluids in microfluidic systems. The technique is based on the fluid dynamics of Taylor flow in microchannels, where bubble velocity and liquid film thickness,as shown in Fig. 5(e) are measured by a high-speed video camera and a laser confocal displacement meter (LFDM), and thus the interfacial tension and viscosity are calculated from theoretical equations. This technique shows good results for a specific range of flow rates and concentrations, although the uncertainty in bubble deformation and liquid film thickness measurements may lead to large measurement errors. Pham et al. [79] proposed a way to measure viscosity based on the ideal gas law, whereby the pressure drop in a laminar flow in a capillary tube is directly proportional to the viscosity of the fluid according to the Hagen-Poiseuille equation. They derived the viscosity indirectly by measuring the change in volume of enclosed air and successfully performed viscosity measurements on a number of different fluids (tap water, acetone, milk 2 % fat, glycerin 30 % and glycerin 40 %). The results showed that the measurements of the liquids were highly consistent with known viscosity values, except for acetone, which is more volatile, and the errors were kept within 4 %. The method is simple in design and uses common laboratory materials, making it a low-cost, easy-to-handle scientific tool.

2.2. Optical tweezers

Optical tweezers technology utilizes a highly focused laser beam to precisely manipulate micro- and nanoscale particles at the microscale by tightly focusing the laser beam using a high numerical aperture (NA) objective lens to form an optical trap, which enables the trapping and manipulation of particles such as cells, biomolecules, dielectric microspheres, and carbon nanotubes [85,86]. This technique provides a non-invasive manipulation method that facilitates the study of biomolecule interactions in complex system interactions of biomolecules in complex systems and enables precise manipulation of micro- and nano-particles [87]. This includes its non-invasiveness, high-precision manipulation capability, broad sample applicability, real-time monitoring ability, and excellent flexibility and scalability [88].

2.2.1. Principle of viscosity measurement by optical tweezers

Optical tweezers use the force generated by an intensely focused light beam to capture and move objects with sizes ranging from tens of nanometers to tens of micrometers [89]. Such as micron-sized particles, microorganisms, and other tiny objects. The principle of operation is based on the phenomena of reflection, refraction and scattering after the interaction of a light beam with particles, which lead to changes in the momentum and angular momentum of the beam, thus generating the optical force. The optical force consists of two main components: one is the scattering force caused by the reflection of particles, and the other is the gradient force generated by the uneven distribution of light intensity. When these two forces reach an equilibrium state at a specific location in the light beam, the particles can be stably captured. Optical tweezers are regarded as the most accurate tool in the microscopic world because of their contactless, low-damage and high-precision characteristics. In particular, when the diameter of the particles captured by optical tweezers is larger than the wavelength of light, the particles exhibit Mie scattering properties. In this case, the force exerted by the optical tweezers on the particles consists not only of a scattering force along the direction of light propagation, but also of a gradient force with axial and radial components. These two components reach equilibrium in the stable trapping region around the focus of the beam: gravity, buoyancy,

the axial component of the gradient force, and the scattering force cancel each other in the vertical direction; while in the transverse plane, the radial component of the gradient force interacts with the horizontal component of the drag force. In a single-beam gradient light trap, the gradient force pulls the captured particles towards the focal point so that they are dynamically driven by the beam in the horizontal plane [90]. The trapping force F_{trap} can be expressed as

$$F_{trap} = \frac{nQP}{c} \tag{7}$$

where Pis the capture laser efficiency, nis the refractive index of the medium, cis the speed of light, and Q is the optical capture rate. When capturing particles in a liquid environment, the resistance to particle movement in the liquid is directly related to the viscosity of the liquid. By adjusting the intensity and shape of the beam of optical tweezers, the particles reach a dynamic equilibrium state in the liquid, at which time the optical force on the particles is equal to the resistance generated by the viscosity of the liquid, so that the viscosity of the liquid can be calculated by measuring the optical force.

2.2.2. Specific examples

The viscosity of a fluid can be measured by tracking the motion of suspended micron-sized particles captured by optical tweezers [91]. A model linking particle escape velocity to fluid viscosity was developed by Zhang et al. [90] Dynamic optical tweezers were used to capture polymethyl methacrylate (PMMA) particles in microtubules, and a galvanometer system was used to reflect the laser beam to form a circular motion, as shown in Fig. 6(a), causing the captured particles to move in a dynamic circular motion. When the liquid resistance is the same as the optical capture force, the particle reaches escape velocity, and the corresponding local solution viscosity is obtained by correspondence. The system has been successfully applied to the viscosity measurement of ethanol and foetal bovine serum (FBS) solutions and can be used for the viscosity determination of biological samples such as sperm and DNA solutions. This will help to advance biomedical research, especially for applications in cell biology and drug delivery. Korzeniewska et al. [92] improved the optical tweezers system for liquid viscosity detection by proposing the oscillatory viscosity measurement technique, which is suitable for liquids with viscosities of up to 2.5mpa. s,and which uses oscillations of the optical trap rather than the movement of the sample stage, which avoids subjecting the sample to vibrations, which are certain sensitive biological samples is particularly important. However, for higher viscosity liquids, consideration of inertial effects may add to the complexity of the measurements due to the increase in Reynolds number. Statsenko et al. [93] constructed a system of optical microscopy combined with optical tweezers, which captures 1μmpolymer beads and moves the captured particles along a short distance of capturing a polymer sphere of 5μm. By recording the captured motion at a selected frequency, as shown in Fig. 6(b), the relationship between the displacement of the captured particles and the viscosity of the medium is proved, and the viscosity of the medium can be well predicted [94]. This method can be applied to the measurement of the viscosity of the intracellular environment, and since cells actively absorb particles, this means that the optical tweezers technology can be used to measure the internal viscosity of the cell, which cannot be achieved by the traditional off-line measurement technology.

Gibson et al. [95] used a CMOS camera to accurately measure the position of the particles captured by the optical tweezers and the applied force. On this basis, Keen et al. [96] employed a holographic optical tweezers technique and successfully captured and tracked multiple particles, the optical path diagram is shown in Fig. 6(c). By analyzing the thermal motion of the particles, they achieved a multi-point measurement of the liquid viscosity in both the frequency and time domains. It is worth noting that calibration with liquids of known viscosity is required to ensure the accuracy of the experimental results. In addition, other researchers have explored indirect methods for viscosity measurements; Yuan et al. [94] used optical tweezers to drive yeast cells or Sio_2 to rotate along a circular track to form a microvortex. The target yeast cells at the center of the vortex would rotate controllably under the effect of viscous forces, thus constructing a cellular micro-motor, and as the viscosity of the surrounding solution increased, the rotational speed of the micro-motor decreased accordingly, thus indirectly establishing a

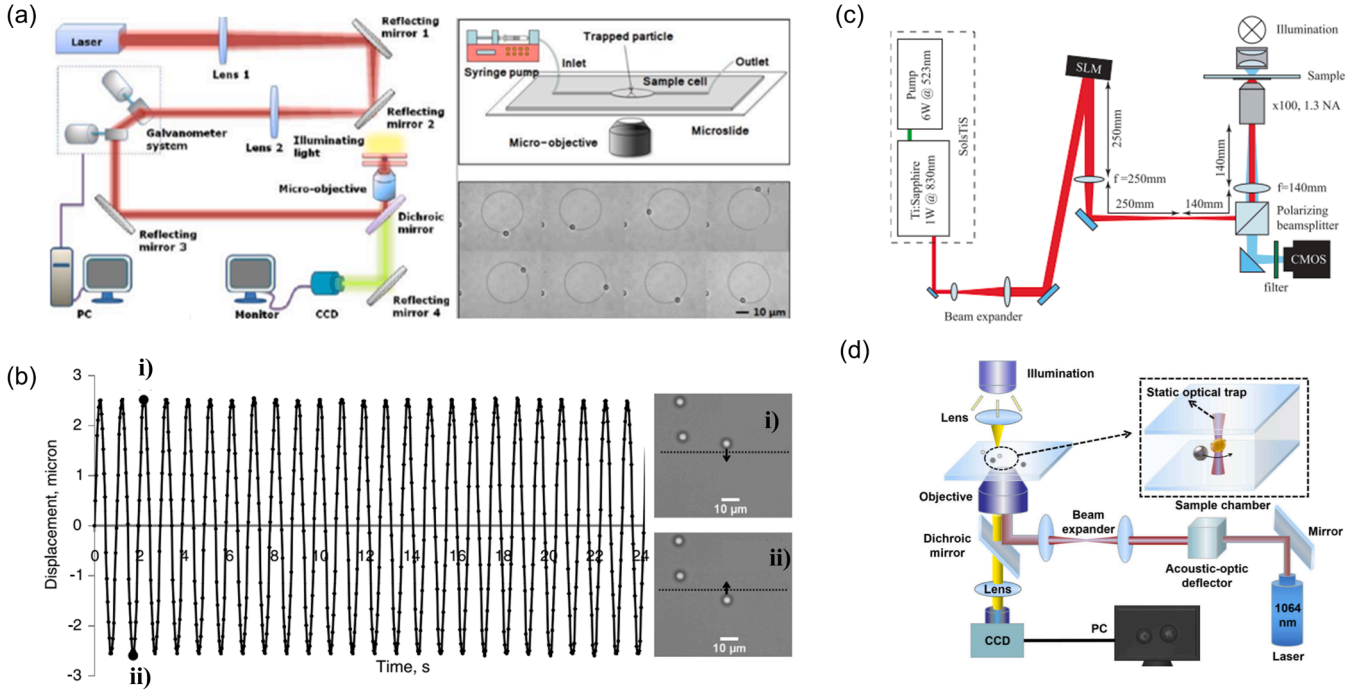

Fig. 6. (a) a schematic of the galvanometer-based optical manipulation system, experimental image of the experimental setup for the rotation of the captured particle along a circular trajectory. (b) position of the manipulated particle. (c) schematic representation of the experiment. (d) Schematic of the experimental setup for viscosity biosensing.

sensing relationship between viscosity and rotational speed, as shown in Fig. 6(d). Hardiman et al. [97] have also used optical tweezers to studied the microfluidic properties of cells in depth. They quantified the interactions between cells and functionalized surfaces and continuously tracked the viscous and elastic changes of cells over several hours. These findings not only enrich our understanding of cell behavior, but also provide new perspectives and methods for research in the biomedical field [98].

2.3. Light scattering technology

Light scattering technology is a powerful complement to viscosity measurement because of its non-invasiveness, high sensitivity and ability to provide real-time data. Here we present two techniques that use the principle of light scattering to probe the dynamic properties of fluids. Surface light scattering viscometry is a method of measuring viscosity using the property of light scattering on the surface of a fluid. When a light beam strikes the surface of a fluid, it produces specific scattering patterns on the surface due to surface tension and fluid viscosity. By analyzing these scattering patterns, the viscosity of the fluid can be deduced. The Surface Light Scattering (SLS) technique can be used to study the surface properties of new materials, such as nanoparticles and polymers, as well as the dynamic properties of biological interfaces such as cell membranes and protein layers. Dynamic Light Scattering (DLS) is a method of measuring the size distribution and motion properties of particles by analyzing the correlation function of the intensity of the scattered light as a function of time, which uses a laser to irradiate a sample. When the laser passes through the sample, part of the light is scattered by the particles in the sample, and then information about the size and distribution of the particles is obtained by detecting the changes in this scattered light. It can be used to study particle size distribution [99] liquid viscosity [100], and diagnosis-related diseases [101], etc. Dynamic light scattering techniques can be used to study the viscosity of polymer solutions, the kinetic properties of colloidal systems, and so on. For example, by measuring the dynamic viscosity of a transparent liquid, the fluidity and shear response properties of the liquid can be evaluated, and the advantages of this technique are its non-invasive nature, the lack of sample preparation, and its ability to provide rapid results.

2.3.1. Viscosity measurement principle of light scattering technology

The Surface Light Scattering (SLS) technique is based on the theory of surface waves at the gas-liquid interface and determines the viscosity of a liquid by measuring the dispersion equation of the surface waves of the fluid. Thermally excited capillary fluctuations on the surface of a liquid or at the liquid-gas interface. These fluctuations are caused by the thermal motion of the liquid molecules and are detected by scattering light. The SLS technique allows the determination of the dynamic viscosity and surface tension of a liquid by measuring the frequency and attenuation of the surface fluctuations. The dispersion equation for surface waves can be expressed as [102]:

$$\left(\mathrm{i}\alpha+\frac{2\eta \mathrm{q}^2}{\rho}\right)^2+\frac{\sigma \mathrm{q}^3}{\rho}+\mathrm{gq}-\frac{4\eta^2\mathrm{q}^4}{\rho^2}\sqrt{1+\frac{\mathrm{i}\alpha\rho}{\eta \mathrm{q}^2}}=0 \tag{8}$$

where gis the gravitational acceleration, $\alpha$is the complex frequency, $\alpha = \pm\omega + \mathrm{i}\Gamma$, $\omega$is the circular frequency of the surface wave, $\Gamma$is the full width of the half peak of the surface wave spectrum, $\Gamma = 1/\tau_c$, $\tau_c$is the relaxation time of the surface wave, η, $\sigma$and $\rho$are the dynamical viscosity, surface tension, and density of the fluid, respectively; and the modulus of the wave vector of the surface vibration mode, $\mathrm{q} = 2\pi\sin\Theta/\lambda_\mathrm{A}$, $\Theta$is the angle of incidence, and $\lambda_\mathrm{A}$is the wavelength of the surface wave of the fluid. This indicates that the viscosity of the fluid can be determined by measuring the frequency of the surface waves. It also reflects that the SLS-based assessment of dynamic viscosity requires knowledge of the density of the fluid.

The approximate solution of the surface wave dynamics at the liquid-vapour interface can be simplified from (8) to be expressed by the following equation.

$$\mathrm{D(S)} = \mathrm{Y} + (1+\mathrm{S})^2 - \sqrt{1+2\mathrm{S}} = 0 \tag{9}$$

Yis a defined dimensionless number, and S is the surface wave contrast frequency. SLS focuses on fluctuations at the surface of a liquid or at a liquid-gas interface, whereas DLS is usually concerned with the Brownian motion of particles in liquids.

The Dynamic Light Scattering (DLS) technique is an effective method for measuring the size of particles by analyzing the Brownian motion of particles in a dispersed system and can also be used to determine the hydrodynamic size of particles. During a DLS measurement, when a laser beam is directed at a particle in a dispersed system, the particle generates an optical signal due to scattering. The intensity of the scattered light should be stable when the particles are at rest. However, in practice, the intensity of the scattered light fluctuates over time due to the Brownian motion of the particles. The degree of this fluctuation is related to the size of the particle: the smaller the particle, the more violent its Brownian motion, and the more pronounced the fluctuation in the intensity of the scattered light. The Stokes-Einstein equation (Stokes-Einstein equation) provides us with a way to extrapolate the viscosity of a liquid from the diffusion behavior of the particles, and the equation can be expressed as [103]:

$$\mathrm{D} = \frac{\mathrm{KT}}{6\pi\eta \mathrm{R}} \tag{10}$$

Where, Dis the diffusion coefficient, Kis the Boltzmann constant, T is the absolute temperature, $\eta$is the viscosity of the medium liquid, Ris the radius of the diffusing particle. From the equation, it is stated that for a given temperature, particle and solution, the diffusion coefficient depends on the viscosity of the liquid to be measured and the radius of the particle, which means that by measuring the radius of diffusion of the particle, we can indirectly derive the viscosity of the liquid [104]

2.3.2. Specific examples

The SLS technique requires that the sample materials are such that they are capable of producing detectable fluctuations at the liquid-gas interface, which includes a wide variety of liquids such as water, oil, and other organic solvents. Measurements of toluene viscosity and surface tension have been accomplished using SLS [105] by Fröba et al. with an overall uncertainty in the results of less than 1 %. SLS allows viscosity to be determined in macroscopic thermodynamic equilibrium without the need for a calibration procedure using a fluid of known viscosity, providing a means of making highly accurate measurements compared to traditional methods such as the falling ball method, the capillary method, and the rotational method, which contributes to improved accuracy and reliability. Later [105] they used the SLS technique to measure the viscosity of diisodecyl phthalate (DIDP), a potential candidate for a medium-high viscosity industrial standard, achieving an uncertainty of less than 1.4 %. With the advancement of optical technology and data processing algorithms, the accuracy and operational simplicity of the SLS technique is expected to be further improved. The SLS approach also supports the measurement of interfacial tension and viscosity in multiphase systems [106], but of course, advanced signal analysis techniques are required to distinguish the scattered signals from different interfaces in order to improve the reliability of multiphase systems. Later Koller et al. [107] investigated the viscosity and interfacial tension of n-heptane (n-heptane) when dissolving carbon dioxide (CO2) at temperatures ranging from 298 to 473 K and saturation pressures up to 5.5 MPa.

Under the same experimental equipment conditions, the team measured the viscosity and surface tension of four n-alkanes, n-hexane, n-octane, n-decane, and n-hexadecane, at thermodynamic equilibrium, over a temperature range from 283.15 K to 573.15 K. During the

experiments, helium was used as a gas source for the dissolution of n-heptane. The helium was used as an inert gas to ensure that the samples were not contaminated during the experiments and to help maintain stable experimental conditions [108]. The SLS method requires a high degree of purity of the samples and ambient conditions, or in some cases may require a longer measurement time. The team has since proposed a new evaluation method to more accurately deal with the effects of rotational flow in the bulk of the fluid in the SLS signal, especially when surface fluctuations approach critical damping [109].

For dynamic light scattering techniques. He et al. [110] presented a method for high-throughput measurement of the viscosity of concentrated protein solutions using a dynamic light scattering (DLS) system. They used polystyrene beads of known size as a spherical tracer and calculated the viscosity of the protein solution indirectly by measuring the radius of the bead particles using the Stokes-Einstein equation. The method was in good agreement with the results from a cone-plate viscometer and showed significant time and material saving advantages for solutions with high protein concentrations, and the DLS method offers the possibility of developing early viscosity analyses. In addition, they found that the addition of calcium ions significantly reduced the viscosity of highly concentrated protein solutions, suggesting that solution viscosity is closely related to intermolecular interactions.Gilroy et al. [111] developed a new method for measuring the viscosity of aqueous DNA solutions using DLS. They succeeded in determining the dynamic viscosity of the solution by measuring DLS data for a series of particles of known size. It was found that as long as the particles were negatively charged and not bound to DNA, dynamic light scattering could be used to measure highly concentrated DNA sample solutions. Compared with the traditional U-tube viscometer, the DLS method is simple to operate at different temperatures, the data accuracy is high, and the samples can be recovered for subsequent experiments. This approach provides a new and accurate method for the application of DLS technology in particle size determination and solution viscosity analysis. Garting et al. [112] realized the measurement of zero shear viscosity of protein by observing the Brownian motion of PEGylated tracer particles embedded in protein solution. This shows that the microrheology based on dynamic light scattering (DLS) can avoid disturbing surface effects compared with classical rheology, and the amount of protein required is greatly reduced. This is of great significance for the pharmaceutical industry and other fields that require precise control of the viscosity of protein solutions. Gazi et al. [113] used a DLS-based microrheology approach used a DLS-based microrheology approach to measure the supersaturated lactose solution and this approach can be expanded to other systems.

2.4. Fiber optics

Optical fiber, as a highly efficient medium for transmitting optical signals, occupies a pivotal position in the field of modern communication technology due to its low energy consumption, high-speed transmission capability, and excellent anti-electromagnetic interference performance [114]. In addition to applications in the communication industry, optical fiber sensors are also widely used to detect a wide range of physical quantities, including, but not limited to, pressure [115-117], displacement [118,119], and electric current [120], due to their unique physical and optical properties. The operating principle of fiber-optic sensors is mainly based on the propagation properties of light and detects changes in the external environment by monitoring the changes in light as it travels through the fiber. Such sensors are highly sensitive and accurate, providing reliable measurements in a variety of complex environments. Owing to their sensitivity to environmental changes, optical fiber sensors also demonstrate immense potential in the measurement of viscosity.

2.4.1. Viscosity measurement principle in optical fiber

Optical fibers usually consist of two parts: the core of the fiber and the cladding. The core is usually made of a material with a high refractive index (e.g. high purity silicon dioxide), while the cladding is wrapped in a material with a low refractive index (usually fluoride or plastic) to keep the optical signal transmitted within the core by the principle of total reflection. The principle of viscosity measurement by fiber optic technology is mainly based on the effect of optical fibers on the propagation properties of light under specific conditions and the physical phenomena that occur when optical fibers interact with fluids.

2.4.2. Specific examples

A fiber grating is a grating structure fabricated in the core of an optical fiber. A long-period fiber grating (LPFG) is a structure that periodically modulates the refractive index along the axis on the core of a single-mode optical fiber and is extremely sensitive to changes in the refractive index of the surrounding medium [121]. When the LPFG sensor is immersed in a fluid, the change in the refractive index of the fluid causes a shift in the resonant wavelength of the grating. By measuring this wavelength shift, the viscosity of the fluid can be inferred [122]. Wang et al. [123] implemented the measurement of asphalt binder using a LPFG as a level sensor. Horan et al. [124] a hollow-core photonic crystal fiber (HC-PCF)-based viscometer to measure liquid viscosity was used to determine liquid viscosity by monitoring the change in propagation characteristics of the liquid as it flowed through the core of the fiber driven by capillary action, as shown in Fig. 7(a). This method allows viscosity measurements to be made using very small sample volumes (down to 10nL)and is therefore suitable for situations where nanoscale aliquots of samples are required. The HC-PCF Viscometer can be easily integrated with a Raman scattering system, as shown in Fig. 7(b), allowing simultaneous analysis of viscosity and Raman spectroscopic information, providing information about the molecular fingerprint of the liquid under study. This is of great importance in areas where small sample volumes need to be analyzed quickly and accurately. Ma et al. [125] proposed an innovative liquid viscosity measurement system that combines a micro 3D printed parallelogram flexible hinge structure (PFHS) and a fiber-optic sensor. The fiber optic sensor is then used to non-contactly measure the vibration amplitude and phase response of the PFHS, which decreases with increasing viscosity and changes the phase response. By fitting the theoretical model and experimental data, this method can not only measure the viscosity, but also evaluate the elastic properties of the liquid.

The application of optic fiber technology in viscosity measurement is mainly due to its ability to perform remote and real-time monitoring, which is particularly suitable for viscosity measurements at high temperatures, high pressures, or in hazardous environments [126]. It has a wide range of potential applications in areas such as industrial process control and geological exploration. Qian et al. [127] provided a new idea for the development of fiber optic viscometer, and proposed a viscosity sensing technique based on fiber Bragg grating (FBG). Acousto-optic modulation was generated by acoustic excitation of the FBG, and it was found that the reflectance spectral bandwidth of the FBG decreased with the increase of solution viscosity. A mathematical model between viscosity and spectral bandwidth was established by fitting the experimental data. This sensor avoids the problem of cross-sensitivity between refractive index and viscosity and demonstrates significant advantages in terms of corrosion resistance, real-time monitoring capability, and compatibility with existing optical devices, which foretells its significant commercial value and potential for a wide range of applications in industry and research. Li et al. [128] based on the previous research on fiber optic sensors proposed a novel viscosity measurement method based on previous research on optical fiber sensors, which uses a U-shaped optical fiber as the core component of the sensor, and encapsulates the U-shaped microfiber in a PDMS film,as shown in Fig. 7(c), when the optical microfiber viscosity sensor is immersed in a solution and moves at a certain speed, the liquid with different viscosities will cause the sensor to bend, which will change the bending transmittance of the optical microfiber, as shown in Fig. 7(d). Through

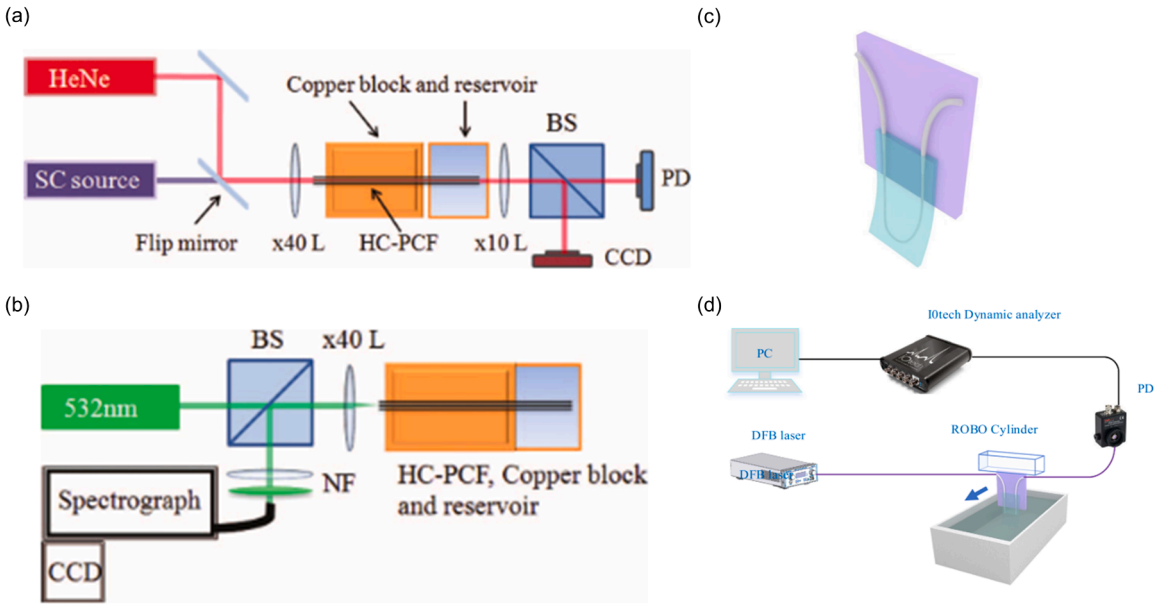

Fig. 7. (a) Schematic of the viscometer experimental setup. (b) Experimental setup for backscattering Raman experiment. (c) Schematic diagram of the optical microfiber U-shaped viscosity. (d) Schematic diagram of the optical microfiber viscosity sensor.

theoretical analyses and experimental measurements, they demonstrated the relationship between the change in transmittance and the viscosity of the solution. This sensor is suitable for the measurement of a wide range of viscosity liquids, but for higher or lower viscosity liquids, further optimization of the sensor design may be required. This optical microfiber-based approach provides a promising solution for practical and cost-effective viscosity measurements.

2.5. *Spectroscopy*

As a powerful analytical tool, spectroscopic techniques support non-destructive and rapid detection, which can be used to predict the composition of substances and even to infer the viscosity of liquids [129]. Although different spectroscopic techniques are based on different physical principles, they share the common goal of revealing the chemical composition and physical properties of liquids by analyzing their absorption, emission, or scattering behavior of light at specific wavelengths [130].

2.5.1. *Viscosity measurement principle by spectroscopy*

The principle of viscosity measurement by spectroscopic techniques mainly relies on the spectral changes produced by the sample after absorbing light of a specific wavelength, and the viscosity value of the sample is inferred by analyzing these spectral changes. Different spectroscopic techniques (e.g., near-infrared spectroscopy, mid-infrared spectroscopy, ultraviolet spectroscopy, etc.) can be used to select the appropriate method for accurate viscosity measurement according to the characteristics of the sample and the measurement needs. The accuracy and range of application in viscosity prediction modelling are limited by several factors. These limitations mainly include the complexity of the spectral data, the variation of experimental conditions, the accuracy of the reference data, the number of samples, the variation of temperature, and the complexity of the sample composition.

2.5.2. *Specific examples*

Several researchers have used near-infrared spectroscopy to predict the viscosity of non-Newtonian fluids including biodiesel [131-135], food [136,137], rubber [138], etc. Zhang et al. [139] used mid-infrared (MIR) and near-infrared (NIR) spectroscopy to viscosity were predicted. It enables the indirect measurement of viscosity by analyzing the absorption and scattering properties of light from the sample. Compared to other optical methods, the spectroscopic technique stands out for its rapidity and non-destructive nature. A viscosity prediction method based on partial least squares regression (PLSR) model was developed by analyzing a large data set. The results showed that both MIR and NIR spectroscopy can be used to accurately predict the viscosity of biodiesel-diesel blends, but NIR spectroscopy provided more accurate results. Haroon et al. [140] presented a new method for online prediction of shampoo viscosity using near-infrared (NIR) spectroscopy, which is relatively new in the personal care product manufacturing process. The method utilizes near infrared (NIR) spectroscopy combined with multivariate statistical analysis, specifically partial least squares (PLS), to predict shampoo viscosity. Subsequently, the team [141] implemented an on-line vibrational spectroscopy technique for use as an alternative to traditional viscosity measurements. They used in-line fiber to couple three probes to achieve the measurement of different spectral techniques, which are the transmission probe for NIR near-infrared measurement, the attenuated total reflection (ATR) probe for MIR, and the backscatter probe for Raman. All three techniques can be applied individually to predict the viscosity of micellar liquids with similar prediction errors. Although these techniques are typically used for compositional analysis, their potential for viscosity measurement is also demonstrated, thus extending the range of applicability of these spectroscopic techniques. The authors also explored the possibility of data fusion by combining datasets from different spectroscopic techniques and found that the NIR-MIR-Raman model, which is based on signal-to-noise ratio weighting, performed best in terms of predictive performance. This finding provides a new perspective on viscosity measurement in industrial processes and may promote the application of these spectroscopic techniques in other fields.

2.6. *Fluorescence*

The fluorescence technique is extremely sensitive and can detect very low concentrations of substances. This makes it particularly important in measuring small changes in viscosity in trace or dilute samples. Changes in the fluorescence intensity of fluorescent probes are sensitive to changes in viscosity [142], allowing even very small changes in viscosity to be accurately detected and recorded. Combined with fluorescence microscopy and other advanced imaging techniques,

researchers can directly observe and track changes in viscosity in different regions of the cell in real time. This capability is extremely important for an in-depth understanding of the substance transport mechanisms and metabolic processes inside the cell, which not only helps to reveal the microscopic basis of cellular functions, but also provides new perspectives and methods for the study of related diseases and the development of drugs [143,144].

2.6.1. Principle of viscosity measurement by fluorescence

The application of fluorescence technology to the measurement of viscosity is based on the sensitivity of fluorescent probes to environmental changes. Fluorescent probes respond to changes in their surrounding microenvironment through specific photophysical or photochemical processes, where viscosity, as a key factor, significantly influences fluorescence performance. The relationship between fluorescence intensity and environmental viscosity can be described by a mathematical model.

$$\tau = zk_0\eta^{\alpha} \tag{11}$$

where k_0 is the radiation rate constant, $\alpha$and zis a constant, τ is the fluorescence lifetime, and η is the viscosity. This method of measurement is particularly suitable for biological systems, as it can be accurately measured by developing fluorescent probes that are specifically tailored to different cell types. In this way, researchers can obtain detailed information about the viscosity inside and outside the cell, which is of great value in understanding cell function and biological processes.

2.6.2. Specific examples

The development of fluorescent bioprobes has overcome many of the challenges in monitoring living organisms, cells, and subcellular structures using optical bioimaging instruments [41] Liu et al. [145] constructed a novel fluorescent probe, ND-1, which has demonstrated significant advantages in viscosity detection in biological systems thanks to its large stokes shift and deep red properties. Marina et al. [143] used a molecular rotor to detect fluorescence lifetimes by laser confocal microscopy as a method to measure the viscosity of living cells. Ponjavic et al. [146] proposed a new in situ viscosity measurement technique, which is suitable for the measurement of liquid viscosity under high-pressure and high-shear condition. Based on the fluorescence lifetime quantification method of fluorescent dye Thiofavin T (ThT), the viscosity change is sensitively detected by measuring the fluorescence lifetime of the fluorescent dye, and successfully applied to the measurement of two model liquids. This technique provides us with an insight into the state of liquids in heterogeneous and high-pressure confinement systems by measuring local viscosity.

Parker et al. [147] employed the Time-Dependent Fluorescence Anisotropy (TDFA) technique to measure the mass transport of complex solutions by monitoring the mass transport of fluorescent tracer particles under steady state flow conditions. Arosio et al. [148] demonstrated a microfluidic platform to measure the viscosity of complex solutions by monitoring the mass transport of fluorescent tracer particles under steady-state flow conditions. These techniques enable non-invasive measurements of flow rates and liquid properties in micro- and nanofluids. Meanwhile, Carroll [149] used a confocal microscopy technique to achieve accurate measurements of fluid viscosity by tracking the dynamics of photobleaching of fluorescent dyes in microfluidic channels. They employed fluorescence recovery after photobleaching (FRAP), in which the fluorescent dye is partially bleached by focusing a laser beam on a specific region of the channel. The bleached dye becomes inert resulting in the inability to fluoresce, and by analyzing the diffusion coefficient of the dye, information about the viscosity of the fluid can be deduced. In addition, Allmendinger et al. [150] proposed a high-throughput viscosity measurement method based on capillary electrophoresis, in which a capillary is filled with a test sample and a constant pressure is applied. By introducing a riboflavin dye into the capillary and monitoring the movement of the protein sample through it, they were able to convert the migration time of the riboflavin dye peak to a viscosity value.

3. Conclusions and perspectives

The application of optical technology has evolved into an efficient and comprehensive method in the field of viscosity measurement. It provides a diverse range of solutions for viscosity testing through different pathways and manufacturing techniques, combined with advanced optical inspection means.

Table 1 in this paper provides a systematic overview of many optical techniques they are based on, classified according to the optical technology they are based on, such as optical microfluidics, dynamic light scattering, optical tweezers, fiber optics, spectroscopy technology and fluorescence. The table provides an exhaustive list of the performances of these optically based viscometers, including, but not limited to viscosity measurement range, the volume of samples required, the materials used, and the accuracy of the measurements. By integrating the content of the table with specific examples, we can clearly appreciate that these optical-based viscosity measurement methods are capable of flexibly adapting to various measurement conditions and meeting diverse viscosity measurement requirements. The unique feature of optical technology is its non-contact measurement method, which does not interfere with the flow characteristics of the solution and provides great convenience for the study of the viscosity of fluids with complex rheological behaviors.

3.1. Applicability of various optical methods

When exploring optical measurement methods for liquid viscosity, we need to not only focus on their innovative potential, but also gain a deeper understanding of each technique's practical application considerations. This review will provide a comprehensive assessment of macrosopic Optical imaging Microfluidics, as well as localized microscopic techniques, optical tweezers, light scattering techniques, optical fiber, spectroscopy and fluorescence technologies in terms of their advantages, technological limitations, difficulties, costs, and prospects for future development, in order to reveal their practical application value in viscosity measurement.

Optical imaging Microfluidics provides a precise method for viscosity measurement at the macro level. By exerting precise control over fluid flow within microfluidic chip, the technique enables rapid offline measurement of the overall viscosity value of a solution. This method is favored for its high accuracy and wide applicability, typically being able to control measurement errors to within 5 %. A significant advantage is that no direct contact with the sample is required, thus avoiding potential contamination risks. In addition, the ability of Optical imaging Microfluidics to deliver measurements quickly makes it particularly effective in application scenarios that require a fast response time [151]. Nonetheless, the application of this technology may be limited by the need for complex microfluidic chip designs and sophisticated equipment, which may hamper its spread to a wider range of settings. The development and production of microfluidic chips may be costly and require high precision optical inspection systems. Development and production of microfluidic chips may be costly. For the initial chip substrate design, the cost consumption is high. Although the initial investment is large, the cost can be equalised by later stages. However, 3D printing microfluidic technology is now becoming mature enough to support the processing of complex microfluidic chips [152]. So Optical imaging Microfluidics is a powerful tool that is valuable for viscosity measurement research and industrial applications. In contrast, other optical methods approach from a microscopic perspective of the liquid, exploring the interactions between the liquid and light as well as microscopic particles to achieve indirect viscosity measurements.

Table 1
Overview of the optical viscometers reviewed here.

Optical Viscometer	Name	Observational tools	Materials	Volume	Viscosity Range	Errors	Drawbacks	Ref.
Optical imaging Microfluidics	Nanoliter Viscometer	Olympus SZX12 stereomicroscope	Silicon glass	600nL	1–5cp	<3 %	Only Newtonian fluids can be measured.	[49]
	Microfluidic Capillary Viscometer	Olympus SZX12 stereomicroscope	Silicon glass	1μL	1–600 cp	NA	Shear rate range is limited.	[50]
	Micro-Optofluidic Viscometer	Optical Detection System;	PMMA	26μL	0.5 m Pa·s-50mpa.s	<0.5 %	Only Newtonian fluids.	[53]
	iCapillary	smartphone camera	PDMS	NA	10–10000s^{-1}	NA	The test is long, and device is divided into two modules.	[55]
	Inertial viscometer	CMOS camera.Laser speckle contrast imaging.	NA	NA	NA	<2 %	Complex equipment.	[63]
	Microfluidic Viscosimeter	Optical microscopy	PDMS	30μL	2 m Pa·s −70 Pa·s	NA	Assuming the fluid is Newtonian.	[64]
	3D printed microfluidic viscometer	Optical microscope. High-speed camera	3D printed	NA	NA	5 %	There may be some errors when measuring the interface width.	[67]
	Consistent Microfluidic Viscometer	CCD camera.Epi-fluorescence Microscope.	PDMS	NA	NA	<4 %	Complex flow rate control.	[69-73]
	Nanoliter droplet viscometer	Microscope.	glass	30nL	~101 m Pa·s	<6.6 %	Unmeasured non-Newtonian fluid.	[77]
	Droplet-Based Microfluidic Capillary Viscometer	Stereoscopic dissection microscope. Microscope camera. Fluorescence detector.	PDMS;glass capillary	NA	0.96–52 cp	0.1 %	The high viscosity sample has a large droplet spacing.	[79]
	water-in-oil Continuous viscometer	Inverted microscope. CCD camera.	glass	< 1μL	$0.01\mu_{oil}$ − $10\mu_{oil}$	<5 %	The measured value depends on the oil phase.	[80]
	High throughput analysis	Inverted microscope. ×20 microscope. High-speed camera	PDMS	NA	20 m Pa·s −500 m Pa·s	NA	Non-Newtonian fluid is not discussed.	[83]
Optical tweezers	A dynamic optical tweezers system	The galvanometer-based optical manipulation system. Mirror galvanometer systems. Fiber laser	PMMA particle	< 30μL	NA	NA	Need to know the refractive index of the surrounding medium.	[90]
	Optical tweezers combined with optical microscopy	Optical microscope. Optical tweezers. NIR laser. CMOS camera.	1μm polymer spheres	NA	1 cp - 4 cp	NA	At high frequencies, the detection of small displacements may be limited by the camera resolution.	[93]
DLS	High-throughput dynamic light scattering method	DLS	51–250 nm polystyrene beads	NA	NA	NA	At high protein concentrations, strong light scattering signals from protein molecules may interfere with the measurement.	[110]
Fiber optics	Hollow core photonic crystal fiber	Supercontinuum source (SC). HeNe laser.Optical microscope. CCD camera.Optical spectrum analyzer (OSA).Andor spectrometer.	HC-PCF-1060	<10 nL	NA	NA	Complex system setup.	[124]
	Fiber-Optic Sensor	Fiber optic sensor	3D printing material (RGD525)	NA	1–1045 m Pa·s	<3.7 %	Need to know the density of the liquid to be measured	[125]
	U-shaped optical microfiber	DFB laser	PDMS;optical microfiber	NA	10–50 m Pa·s	<3.8 %	Non-Newtonian fluid is not discussed.	[128]
Fluorescence	Capillary electrophore-sis	ProteomeLab PA CE 800 instrument	Bare fused-silica capillaries	NA	5–40 m Pa·s	NA	High viscosity samples may lead to irregular shape of dye peaks and affect the accuracy of measurement.	[150]

Optical tweezers technology is suitable for biomolecule research because it can be manipulated without touching the sample, thus avoiding physical damage to the sample [153]. The optical tweezers technique relies on tiny particles in solution for measurements and is therefore limited by the optical properties of the sample solution and the concentration of the particulate matter, and is only applicable to particles that can be captured by the optical tweezers. The optical tweezers method needs to be operated in conjunction with a microscope, requires high precision and stability of the equipment, requires transparent or semi-transparent samples, and has specific requirements for optical properties. Prolonged exposure to high-intensity lasers may result in thermal or photochemical damage [154] to the sample, especially in biological samples. Optical tweezers equipment is costly and requires specialized optical platforms. The method allows for high precision measurements with small numbers of samples and is suitable for laboratory research. It has great potential in cell biology, drug discovery [155] and disease mechanism research. As an advanced micromanipulation tool, optical tweezers technology is promising for future research and industrial applications, despite some challenges and cost issues.

There are various methods of measuring liquid viscosity using light scattering techniques, among which surface light scattering allows non-invasive and non-destructive testing. It provides detailed information on surface properties, thus avoiding the problems of sample contamination and damage that can be caused by traditional contact measurements. It is possible to measure not only liquid viscosity but also other physical properties such as surface tension at the same time [156]. However, the

operational complexity of the surface light scattering technique and its dependence on commercially available instrumentation constitute a notable difficulty of the method [109]. In addition, the high demands on the experimental environment, such as sensitivity to vibrations and air currents, further add to the difficulty. Accurate light sources and detectors are necessary, while data analysis often relies on complex mathematical models. Although equipment costs can be high, especially with the need for high quality lasers, the accuracy and stability of measurements have been significantly improved with significant improvements in key equipment in surface light scattering systems such as lasers, photon counters and digital correlators. These technological advances have not only advanced the application of surface light scattering techniques in laboratory research, but have also broadened their applicability to extreme conditions, such as the study of viscosity and surface tension of binary ionic liquid mixtures in high vacuum environments [157]. The application of this method under extreme conditions demonstrates its wide applicability and flexibility. It has a wide range of applications in surface science, materials science and environmental monitoring [109].

The high sensitivity and resolution of the DLS technique enables the measurement of small changes in viscosity, which is advantageous in application scenarios where high precision measurements are required. In addition, DLS technology is not limited by the transparency of the sample and can be used for viscosity measurements of a wide range of fluids. DLS is mainly used to measure the particle size and size distribution in dispersed systems [158]. DLS has certain requirements on the optical properties of the sample, and requires sufficient scattering intensity. At high concentrations or large particle sizes, the accuracy of DLS may be compromised. Although the DLS technique has significant advantages in terms of accuracy, the results are affected by factors such as sample temperature and concentration and need to be corrected appropriately. The DLS technique usually requires a long data acquisition time to obtain sufficient statistical information, and a large amount of data needs to be processed and analyzed, which adds to the overall time cost of the measurement process. Although modern computer technology has dramatically increased the speed of data processing, DLS measurements still require a long time to complete data analysis and output of results. DLS technology can be applied to multiphase systems such as emulsions and suspensions, providing valuable information about the interaction between dispersed and continuous phases.

Fiber optic technology is suitable for remote and in-situ measurements and is flexible enough to be integrated into other monitoring systems. Non-invasive measurement for hazardous or hard-to-reach environments. Fiber grating based viscosity measurement methods require accurate wavelength detection and data processing and are sensitive to environmental factors such as temperature and pressure. Precise optical alignment and signal detection are required. The application of fiber optic technology in viscosity measurement is characterized by its ability to perform remote and real-time monitoring, which is particularly suited to viscosity measurements at high temperatures, high pressures, or in hazardous environments [159]. It has a wide range of potential applications in areas such as industrial process control and geological exploration. The trend towards miniaturisation and integration of fiber optic sensors will drive their application in more fields.

Spectroscopic techniques have the advantage of being non-destructive and are suitable for the analysis of sensitive samples [160]. By combining multiple spectral data, the predictive power of models can be significantly improved. However, in some cases, spectroscopic techniques may not perform well due to low signal-to-noise ratios and transmission issues [161]. In addition, spectral data analysis is complex and requires specialized spectral resolution skills. High-quality spectrometers and associated equipment are costly. However, with advances in spectral techniques and data processing algorithms, the accuracy and reliability of predictive models will be further improved [162]. Data fusion models combining multiple spectroscopic techniques will provide more comprehensive analyses of sample properties.

Fluorescence techniques determine viscosity indirectly by observing variations in the fluorescence characteristics of molecules within a solution. This method is particularly important in biomedical research and can provide important information about the internal structure and properties of a sample without affecting the biological sample. Fluorescence techniques are capable of making highly sensitive and specific measurements and are suitable for use in studies at the biomolecular and cellular levels. However, this approach necessitates the utilization of fluorescently labeled samples or probes, imposing specific requirements on the stability and specificity of these fluorescent labels. In addition, the complex environment within an organism may interfere with the fluorescence probe [163]. The cost of fluorescence equipment varies by configuration, and the development of novel fluorescent probes may involve high R&D costs. Nonetheless, fluorescent probes play an irreplaceable role from monitoring the dynamics of intracellular proteins [164] to real-time analysis of complex biological processes [165]. With the advancement of technology and the development of novel probes, the application of fluorescence technology in the biomedical field will be more promising [166].

Each optical technique has its unique advantages and limitations in measuring viscosity. The choice of technique depends on the specific needs of the measurement, the characteristics of the sample, the cost budget, and the operational feasibility. Currently, research on optical viscosity measurement techniques is moving towards improving measurement accuracy, expanding measurement range, increasing the scope of applications, and reducing costs to better meet the needs of various industries. Simultaneously, researchers are actively exploring integration of multiple optical technologies for more comprehensive viscosity measurement and analysis. As technology advances and research deepens, through innovation and integration, these optical technologies will play an increasingly important role in the future.

3.2. The development direction of viscosity measurement by optical method

a) Combined with computational optical imaging

Computational Optical Imaging (COI) incorporates cutting-edge knowledge from a variety of fields, including optics, information technology, and mathematics, and foreshadows the future trends in advanced optical imaging technology. This technology has achieved significant breakthroughs from still images to dynamic video to ultra-high-speed, super-resolution, and multidimensional imaging [167]. For some complex fluids, such as those that exhibit viscoelasticity [168], COI is able to provide a more accurate measurement of the viscosity of fluids by means of precise image analysis and processing [169], combined with machine learning and deep learning algorithms, can identify and classify specific patterns and objects in the image, which not only provides more accurate viscosity measurements, but also reveals other physical properties of the fluid, such as surface tension, maximum relaxation time, etc. [62].. This provides more information for comprehensive analyses of fluids. In addition, computational optical imaging technology has greatly broadened human horizons in fields such as biomedical imaging [170], deep space exploration [171], and industrial inspection [172,173].

b) Combined with microfluidic technology

Through microchannels and surface structures, microfluidics can achieve precise manipulation of fluids within a specific restricted scale range, and thus achieve light control of fluid substance properties or modulation of light propagation through the fluid medium [174]. The combination of microfluidics with optical imaging, optical tweezers, fiber optics, and other technologies has led to a wide range of applications in the fields of field detection, such as molecular biology, chemical analysis, and food safety sensing [175].

c) Integrated design and multi-parameter measurement

Optical viscosity measurement technology can be combined with

other types of sensor technology, such as temperature, pressure, concentration sensors, etc., to achieve a comprehensive analysis of the characteristics of fluid samples. By integrating a variety of optical sensors, the information of viscosity, conductivity [176], flow velocity [177], surface tension [178] and other parameters can be obtained at the same time.

CRediT authorship contribution statement

Yan Ge: Writing – review & editing, Writing – original draft, Methodology, Investigation, Conceptualization. **Xingxing Huang:** Writing – review & editing, Methodology, Conceptualization. **Xusheng Tang:** Resources, Investigation, Conceptualization. **Yuntong Wang:** Writing – review & editing, Methodology. **Fuyuan Chen:** Writing – review & editing, Methodology. **Dongyang Xiao:** Conceptualization. **Peng Liang:** Writing – review & editing, Conceptualization. **Bei Li:** Writing – review & editing, Conceptualization.

Declaration of competing interest

The authors declare that they have no known competing financial interests or personal relationships that could have appeared to influence the work reported in this paper

Data availability

No data was used for the research described in the article.

Acknowledgements

This work was financially supported by the National Natural Science Foundation of China (Grant No.62304222)

References

[1] Kim BJ, Lee SY, Jee S, Atajanov A, Yang S. Micro-Viscometer for Measuring Shear-Varying Blood Viscosity over a Wide-Ranging Shear Rate. Sensors (Basel) 2017:17. https://doi.org/10.3390/s17061442.
[2] Shah Z, Raja MAZ, Khan WA, Shoaib M, Tirth V, Algahtani A, Irshad K, Al-Mughanam T. Computational intelligence paradigm with Levenberg-Marquardt networks for dynamics of Reynolds nanofluid model for Casson fluid flow. Tribol Int 2024:191. https://doi.org/10.1016/j.triboint.2023.109180.
[3] Zijlstra N, Mars M, de Wijk R, Westerterp-Plantenga M, de Graaf C. The effect of viscosity on ad libitum food intake and satiety hormones. Appetite 2007;49:341.
[4] Zhang Q, Zhong S, Lin J, Huang Y, Nsengiyumva W, Chen W, Luo M, Zhong J, Yu Y, Peng Z, Cheng S. Anti-noise frequency estimation performance of Hanning-windowed energy centrobaric method for optical coherence velocimeter. Opt Lasers Eng 2020;134:106250. https://doi.org/10.1016/j.optlaseng.2020.106250.
[5] Fernandes M, Sousa LC, António CC, Pinto SIS. Accuracy and temporal analysis of non-Newtonian models of blood in the computational FFR – Numerical implementation. Int J Non Linear Mech 2024;161:104683. https://doi.org/10.1016/j.ijnonlinmec.2024.104683.
[6] Abu-Jdayil B, Mohameed HA, Sa'id M, Snobar T. Rheological characterization of hair shampoo in the presence of dead sea salt. Int J Cosmet Sci 2004;26:19–29. https://doi.org/10.1111/j.0142-5463.2004.00201.x.
[7] Ren Z, Kowalski A, Rodgers TL. Measuring inline velocity profile of shampoo by electrical resistance tomography (ERT). Flow Measurement and Instrumentation 2017;58:31–7. https://doi.org/10.1016/j.flowmeasinst.2017.09.013.
[8] Meier G, Vavrin R, Kohlbrecher J, Buitenhuis J, Lettinga MP, Ratajczyk M. SANS and dynamic light scattering to investigate the viscosity of toluene under high pressure up to 1800 bar. Measurement Science and Technology 2008;19:034017. https://doi.org/10.1088/0957-0233/19/3/034017.
[9] Yang F, Chen Z, Xing D. Single-Cell Photoacoustic Microrheology. IEEE Trans Med Imaging 2020;39:1791–800. https://doi.org/10.1109/tmi.2019.2958112.
[10] Dintenfass L. Blood rheology in cardio-vascular diseases. Nature 1963;199. https://doi.org/10.1038/199813a0. 813-&.
[11] Toprak K, Kaplangoray M, Palice A, Inanir M, Memioglu T, Kok Z, Altiparmak IH, Toprak IH, Bicer A, Demirbag R. Increased whole blood viscosity is associated with primary idiopathic complete atrioventricular block and poor clinical outcomes in these patients. Clin Hemorheol Microcirc 2023;84:141–51. https://doi.org/10.3233/ch-221596.
[12] Chen W, Hu B, Zhang S, Zheng Y, Zhou Z, Mai Y. Relationship between blood viscosity and existence and severity of carotid artery plaque. Clin Hemorheol Microcirc 2023;83:351–8. https://doi.org/10.3233/ch-221597.
[13] Amador J, Hartel R, Rankin S. The Effects of Fat Structures and Ice Cream Mix Viscosity on Physical and Sensory Properties of Ice Cream. J Food Sci 2017;82:1851–60. https://doi.org/10.1111/1750-3841.13780.
[14] Brust M, Schaefer C, Doerr R, Pan L, Garcia M, Arratia PE, Wagner C. Rheology of human blood plasma: viscoelastic versus Newtonian behavior. Phys Rev Lett 2013;110:078305. https://doi.org/10.1103/PhysRevLett.110.078305.
[15] Jiskoot W, Hawe A, Menzen T, Volkin DB, Crommelin DJA. Ongoing Challenges to Develop High Concentration Monoclonal Antibody-based Formulations for Subcutaneous Administration: Quo Vadis? J Pharm Sci 2022;111:861–7. https://doi.org/10.1016/j.xphs.2021.11.008.
[16] Shire SJ. Formulation and manufacturability of biologics. Curr Opin Biotechnol 2009;20:708–14. https://doi.org/10.1016/j.copbio.2009.10.006.
[17] Goswami S, Wang W, Arakawa T, Ohtake S. Developments and Challenges for mAb-Based Therapeutics. Antibodies 2013;2:452–500. https://doi.org/10.3390/antib2030452.
[18] Heise T, Nosek L, Dellweg S, Zijlstra E, Præstmark KA, Kildegaard J, Nielsen G, Sparre T. Impact of injection speed and volume on perceived pain during subcutaneous injections into the abdomen and thigh: a single-centre, randomized controlled trial. Diabetes Obes Metab 2014;16:971–6. https://doi.org/10.1111/dom.12304.
[19] Corach J, Sorichetti PA, Romano SD. Electrical properties and kinematic viscosity of biodiesel. Fuel 2021;299. https://doi.org/10.1016/j.fuel.2021.120841.
[20] Joshipura MH, Saxena P, Shah N, Dwivedi A, Pillai S, Aggrawal M. Determining and modeling of density and viscosity of biodiesel-diesel and biodiesel-diesel-butanol blends. International Journal of Chemical Reactor Engineering 2023;21:1561–9. https://doi.org/10.1515/ijcre-2023-0004.
[21] Kleinschmidt D, Brüning F, Petzke J. Wall Slip-Free Viscosity Determination of Filled Rubber Compounds Using Steady-State Shear Measurements. Polymers (Basel) 2023:15. https://doi.org/10.3390/polym15224406.
[22] Kopal I, Labaj I, Vršková J, Harničárová M, Valíček J, Tozan H. Intelligent Modelling of the Real Dynamic Viscosity of Rubber Blends Using Parallel Computing. Polymers (Basel) 2023:15. https://doi.org/10.3390/polym15173636.
[23] Mayerl CJ, Edmonds CE, Gould FDH, German RZ. Increased viscosity of milk during infant feeding improves swallow safety through modifying sucking in an animal model. J Texture Stud 2021;52:603–11. https://doi.org/10.1111/jtxs.12599.
[24] Cruz C, Arafeh A, Martin PA, Fonte CP, De Simone A, Oppong FK, Jeatt W, Rodgers TL. Assessment of Near-Infrared and Raman Spectroscopy as Analytical Tools to Predict Viscosity of Ice Cream Mixes. Appl Spectrosc 2023;77:764–73. https://doi.org/10.1177/00037028231176824.
[25] Levy G, Jusko WJ. Effect of viscosity on drug absorption. J Pharm Sci 1965;54:219–24. https://doi.org/10.1002/jps.2600540212.
[26] Zidar M, Rozman P, Belko-Parkel K, Ravnik M. Control of viscosity in biopharmaceutical protein formulations. J Colloid Interface Sci 2020;580:308–17. https://doi.org/10.1016/j.jcis.2020.06.105.
[27] Oliveira SM, Neeli-Venkata R, Goncalves NS, Santinha JA, Martins L, Tran H, Mäkelä J, Gupta A, Barandas M, Häkkinen A, Lloyd-Price J, Fonseca JM, Ribeiro AS. Increased cytoplasm viscosity hampers aggregate polar segregation in Escherichia coli. Mol Microbiol 2016;99:686–99. https://doi.org/10.1111/mmi.13257.
[28] Kwapiszewska K, Szczepański K, Kalwarczyk T, Michalska B, Patalas-Krawczyk P, Szymański J, Andryszewski T, Iwan M, Duszyński J, Hołyst R. Nanoscale Viscosity of Cytoplasm Is Conserved in Human Cell Lines. J Phys Chem Lett 2020;11:6914–20. https://doi.org/10.1021/acs.jpclett.0c01748.
[29] Zhang S, Sun Y, Liu W, Feng W, Zhang M, Li Z, Yu M. Coumarin-based fluorescent probes toward viscosity in mitochondrion/lysosome. Anal Biochem 2022;652:114752. https://doi.org/10.1016/j.ab.2022.114752.
[30] Wang D, Gong Z, Huang W, Zhao J, Geng J, Liu Z, Zhang R, Han G, Zhang Z. A viscosity-sensitivity probe for cross-platform multimodal imaging from mitochondria to animal. Talanta 2023;258:124346. https://doi.org/10.1016/j.talanta.2023.124346.
[31] Müller FJ, Pita JC. A simple electronic capillary microviscometer. Anal Biochem 1983;135:106–11. https://doi.org/10.1016/0003-2697(83)90737-6.
[32] Gupta S, Wang WS, Vanapalli SA. Microfluidic viscometers for shear rheology of complex fluids and biofluids. Biomicrofluidics 2016;10:043402. https://doi.org/10.1063/1.4955123.
[33] Ault JT, Shin S, Garcia A, Perazzo A, Stone HA. Viscosity measurements of glycerol in a parallel-plate rheometer exposed to atmosphere. J Fluid Mech 2023;968:A2. https://doi.org/10.1017/jfm.2023.489.
[34] Yu H, Liang L, Yuandong AG. Capacitive micromachined ultrasonic transducer (CMUT) based micro viscosity sensor. Sensors and Actuators B-Chemical 2016;227:346–51. https://doi.org/10.1016/j.snb.2015.12.061.
[35] Smith PD, Young RCD, Chatwin CR. A MEMS viscometer for unadulterated human blood. Measurement 2010;43:144–51. https://doi.org/10.1016/j.measurement.2009.08.011.
[36] Riesch C, Reichel EK, Keplinger F, Jakoby B. Characterizing Vibrating Cantilevers for Liquid Viscosity and Density Sensing. J Sens 2008;2008:1–9. https://doi.org/10.1155/2008/697062.
[37] Puchades I, Fuller LF. A Thermally Actuated Microelectromechanical (MEMS) Device for Measuring Viscosity. Journal of Microelectromechanical Systems 2011;20:601–8. https://doi.org/10.1109/jmems.2011.2127447.
[38] He XS, Liu QX, Huang XC, Chen YM. Dynamic Response Analysis of the Fractional-Order System of MEMS Viscometer. Cmes-Computer Modeling in Engineering & Sciences 2015;108:159–69.

[39] Singh P, Sharma K, Puchades I, Agarwal PB. A comprehensive review on MEMS-based viscometers. Sensors and Actuators A: Physical 2022:338. https://doi.org/10.1016/j.sna.2022.113456.

[40] Farkas DL. Invention and commercialization in optical bioimaging. Nat Biotechnol 2003;21:1269–71. https://doi.org/10.1038/nbt1103-1269.

[41] Wang Y, Li Y, Wei F, Duan Y. Optical Imaging Paves the Way for Autophagy Research. Trends Biotechnol 2017;35:1181–93. https://doi.org/10.1016/j.tibtech.2017.08.006.

[42] Bett F, Brown S, Dong A, Christian M, Ajala S, Santiago K, Albin S, Marz A, Deo M. Optical Deformation of Biological Cells using Dual-Beam Laser Tweezer. Annu Int Conf IEEE Eng Med Biol Soc 2022;2022:17–20. https://doi.org/10.1109/embc48229.2022.9871373.

[43] Dehnaw AM, Manie YC, Du LY, Yao CK, Jiang JW, Liu BX, Peng PC. Integrated Sensor-Optics Communication System Using Bidirectional Fiber and FSO Channels and Hybrid Deep Learning Techniques. Sensors (Basel) 2023:23. https://doi.org/10.3390/s23208434.

[44] Zandvliet HJ, van Houselt A. Scanning tunneling spectroscopy. Annu Rev Anal Chem (Palo Alto Calif) 2009;2:37–55. https://doi.org/10.1146/annurev-anchem-060908-155213.

[45] Whitesides GM. The origins and the future of microfluidics. Nature 2006;442:368–73. https://doi.org/10.1038/nature05058.

[46] Puneeth SB, Kulkarni MB, Goel S. Microfluidic viscometers for biochemical and biomedical applications: A review. Engineering Research Express 2021:3. https://doi.org/10.1088/2631-8695/abfd47.

[47] Sackmann EK, Fulton AL, Beebe DJ. The present and future role of microfluidics in biomedical research. Nature 2014;507:181–9. https://doi.org/10.1038/nature13118.

[48] Chhabra RP. Non-Newtonian fluids: an introduction, school on rheology of complex fluids. Chennai, INDIA: Indian Inst Technol Madras; 2010. p. 3–34.

[49] Srivastava N, Davenport RD, Burns MA. Nanoliter viscometer for analyzing blood plasma and other liquid samples. Anal Chem 2005;77:383–92. https://doi.org/10.1021/ac0494681.

[50] Srivastava N, Burns MA. Analysis of non-Newtonian liquids using a microfluidic capillary viscometer. Anal Chem 2006;78:1690–6. https://doi.org/10.1021/ac0518046.

[51] Han Z, Tang X, Zheng B. A PDMS viscometer for microliter Newtonian fluid. Journal of Micromechanics and Microengineering 2007;17:1828–34. https://doi.org/10.1088/0960-1317/17/9/011.

[52] Morhell N, Pastoriza H. A single channel capillary microviscometer. Microfluid Nanofluidics 2013;15:475–9. https://doi.org/10.1007/s10404-013-1162-4.

[53] Bamshad A, Nikfarjam A, Sabour MH. Capillary-based micro-optofluidic viscometer. Measurement Science and Technology 2018;29. https://doi.org/10.1088/1361-6501/aace7d.

[54] Son Y. Determination of shear viscosity and shear rate from pressure drop and flow rate relationship in a rectangular channel. Polymer (Guildf) 2007;48:632–7. https://doi.org/10.1016/j.polymer.2006.11.048.

[55] Solomon DE, Abdel-Raziq A, Vanapalli SA. A stress-controlled microfluidic shear viscometer based on smartphone imaging. Rheol Acta 2016;55:727–38. https://doi.org/10.1007/s00397-016-0940-9.

[56] Verma MK, Majumder A, Ghatak A. Embedded template-assisted fabrication of complex microchannels in PDMS and design of a microfluidic adhesive. Langmuir 2006;22:10291–5. https://doi.org/10.1021/la062516n.

[57] Zou M, Cai S, Zhao Z, Chen L, Zhao Y, Fan X, Chen S. A novel polydimethylsiloxane microfluidic viscometer fabricated using microwire-molding. Rev Sci Instrum 2015;86:104302. https://doi.org/10.1063/1.4933388.

[58] Oh S, Choi S. 3D-Printed Capillary Circuits for Calibration-Free Viscosity Measurement of Newtonian and Non-Newtonian Fluids. Micromachines (Basel) 2018:9. https://doi.org/10.3390/mi9070314.

[59] Oh S, Kim B, Choi S. A 3D-Printed Multichannel Viscometer for High-Throughput Analysis of Frying Oil Quality. Sensors (Basel) 2018:18. https://doi.org/10.3390/s18051625.

[60] Bilodeau C, Kazakov A, Mukhopadhyay S, Emerson J, Kalantar T, Muzny C, Jensen K. Machine learning for predicting the viscosity of binary liquid mixtures. Chemical Engineering Journal 2023;464:142454. https://doi.org/10.1016/j.cej.2023.142454.

[61] Roosta A, Haghbakhsh R, Rita C. Duarte A, Raeissi S. Deep eutectic solvent viscosity prediction by hybrid machine learning and group contribution. J Mol Liq 2023;388:122747. https://doi.org/10.1016/j.molliq.2023.122747.

[62] Del Giudice F, Barnes C. Rapid Temperature-Dependent Rheological Measurements of Non-Newtonian Solutions Using a Machine-Learning Aided Microfluidic Rheometer. Anal Chem 2022;94:3617–28. https://doi.org/10.1021/acs.analchem.1c05208.

[63] Kornaeva EP, Stebakov IN, Kornaev AV, Dremin VV, Popov SG, Vinokurov AY. A method to measure non-Newtonian fluids viscosity using inertial viscometer with a computer vision system. Int J Mech Sci 2023:242. https://doi.org/10.1016/j.ijmecsci.2022.107967.

[64] Guillot P, Panizza P, Salmon JB, Joanicot M, Colin A, Bruneau CH, Colin T. Viscosimeter on a microfluidic chip. Langmuir 2006;22:6438–45. https://doi.org/10.1021/la060131z.

[65] Goel S, Venkateswaran PS, Prajesh R, Agarwal A. Rapid and automated measurement of biofuel blending using a microfluidic viscometer. Fuel 2015;139:213–9. https://doi.org/10.1016/j.fuel.2014.08.053.

[66] Venkateswaran PS, Sharma A, Dubey S, Agarwal A, Goel S. Rapid and Automated Measurement of Milk Adulteration Using a 3D Printed Optofluidic Microviscometer (OMV). IEEE Sens J 2016;16:3000–7. https://doi.org/10.1109/jsen.2016.2527921.

[67] Hong H, Song JM, Yeom E. 3D printed microfluidic viscometer based on the co-flowing stream. Biomicrofluidics 2019;13:014104. https://doi.org/10.1063/1.5063425.

[68] Kim S, Kim KC, Yeom E. Microfluidic method for measuring viscosity using images from smartphone. Opt Lasers Eng 2018;104:237–43. https://doi.org/10.1016/j.optlaseng.2017.05.016.

[69] Kang YJ, Yoon SY, Lee KH, Yang S. A Highly Accurate and Consistent Microfluidic Viscometer for Continuous Blood Viscosity Measurement. Artif Organs 2010;34:944–9. https://doi.org/10.1111/j.1525-1594.2010.01078.x.

[70] Kang YJ, Yang S. Integrated microfluidic viscometer equipped with fluid temperature controller for measurement of viscosity in complex fluids. Microfluid Nanofluidics 2012;14:657–68. https://doi.org/10.1007/s10404-012-1085-5.

[71] Jun Kang Y, Yeom E, Lee SJ. A microfluidic device for simultaneous measurement of viscosity and flow rate of blood in a complex fluidic network. Biomicrofluidics 2013;7:54111. https://doi.org/10.1063/1.4823586.

[72] Kang YJ, Yeom E, Lee SJ. Microfluidic biosensor for monitoring temporal variations of hemorheological and hemodynamic properties using an extracorporeal rat bypass loop. Anal Chem 2013;85:10503–11. https://doi.org/10.1021/ac402505z.

[73] Kang YJ. Periodic and simultaneous quantification of blood viscosity and red blood cell aggregation using a microfluidic platform under in-vitro closed-loop circulation. Biomicrofluidics 2018;12:024116. https://doi.org/10.1063/1.5017052.

[74] Solomon DE, Vanapalli SA. Multiplexed microfluidic viscometer for high-throughput complex fluid rheology. Microfluid Nanofluidics 2013;16:677–90. https://doi.org/10.1007/s10404-013-1261-2.

[75] Carnicer V, Alcázar C, Orts MJ, Sánchez E, Moreno R. Microfluidic rheology: A new approach to measure viscosity of ceramic suspensions at extremely high shear rates. Open Ceramics 2021:5. https://doi.org/10.1016/j.oceram.2020.100052.

[76] Moragues T, Arguijo D, Beneyton T, Modavi C, Simutis K, Abate AR, Baret JC, deMello AJ, Densmore D, Griffiths AD. Droplet-based microfluidics. Nature Reviews Methods Primers 2023;3. https://doi.org/10.1038/s43586-023-00212-3.

[77] Livak-Dahl E, Lee J, Burns MA. Nanoliter droplet viscometer with additive-free operation. Lab Chip 2013;13:297–301. https://doi.org/10.1039/c2lc41130j.

[78] Wehking JD, Gabany M, Chew L, Kumar R. Effects of viscosity, interfacial tension, and flow geometry on droplet formation in a microfluidic T-junction. Microfluid Nanofluidics 2013;16:441–53. https://doi.org/10.1007/s10404-013-1239-0.

[79] DeLaMarre MF, Keyzer A, Shippy SA. Development of a simple droplet-based microfluidic capillary viscometer for low-viscosity Newtonian fluids. Anal Chem 2015;87:4649–57. https://doi.org/10.1021/acs.analchem.5b00677.

[80] Li Y, Ward KR, Burns MA. Viscosity Measurements Using Microfluidic Droplet Length. Anal Chem 2017;89:3996–4006. https://doi.org/10.1021/acs.analchem.6b04563.

[81] Mena SE, Li Y, McCormick J, McCracken B, Colmenero C, Ward K, Burns MA. A droplet-based microfluidic viscometer for the measurement of blood coagulation. Biomicrofluidics 2020;14:014109. https://doi.org/10.1063/1.5128255.

[82] Zeng W, Fu H. Measurement of fluid viscosity based on droplet microfluidics. Physics of Fluids 2020;32. https://doi.org/10.1063/5.0002929.

[83] Andre E, Pannacci N, Dalmazzone C, Colin A. A new way to measure viscosity in droplet-based microfluidics for high throughput analysis. Soft Matter 2019;15:504–14. https://doi.org/10.1039/c8sm02372g.

[84] Sun Y, Guo C, Jiang Y, Wang T, Zhang L. Online measurements of surface tensions and viscosities based on the hydrodynamics of Taylor flow in a microchannel. Rev Sci Instrum 2016;87:114901. https://doi.org/10.1063/1.4963898.

[85] Halma MTJ, Tuszynski JA, Wuite GJL. Optical tweezers for drug discovery. Drug Discov Today 2023;28. https://doi.org/10.1016/j.drudis.2022.103443.

[86] Buosciolo A, Pesce G, Sasso A. New calibration method for position detector for simultaneous measurements of force constants and local viscosity in optical tweezers. Opt Commun 2004;230:357–68. https://doi.org/10.1016/j.optcom.2003.11.062.

[87] Yang Y, Ren YX, Chen M, Arita Y, Rosales-Guzman C. Optical trapping with structured light: a review. Adv Photonics 2021:3. https://doi.org/10.1117/1.Ap.3.3.034001.

[88] Catala-Castro F, Schaeffer E, Krieg M. Exploring cell and tissue mechanics with optical tweezers. J Cell Sci 2022;135. https://doi.org/10.1242/jcs.259355.

[89] Grier DG. A revolution in optical manipulation. Nature 2003;424:810–6. https://doi.org/10.1038/nature01935.

[90] Zhang Y, Wu X, Wang Y, Zhu S, Gao BZ, Yuan XC. Measurement of the microscopic viscosities of microfluids with a dynamic optical tweezers system. Laser Phys 2014;24:065601. https://doi.org/10.1088/1054-660x/24/6/065601.

[91] Heller I, Sitters G, Broekmans OD, Farge G, Menges C, Wende W, Hell SW, Peterman EJ, Wuite GJ. STED nanoscopy combined with optical tweezers reveals protein dynamics on densely covered DNA. Nat Methods 2013;10:910–6. https://doi.org/10.1038/nmeth.2599.

[92] Korzeniewska AK, Drobczyński S. Local measurement of liquid viscosity in optical tweezers. Opt Lasers Eng 2023:164. https://doi.org/10.1016/j.optlaseng.2023.107516.

[93] Statsenko A, Inami W, Kawata Y. Measurement of viscosity of liquids using optical tweezers. Opt Commun 2017;402:9–13. https://doi.org/10.1016/j.optcom.2017.05.034.

[94] Yuan S, Zheng Q, Yao B, Wen M, Zhang W, Yuan J, Lei H. Bio-compatible miniature viscosity sensor based on optical tweezers. Biomed Opt Express 2022;13:1152–60. https://doi.org/10.1364/BOE.452615.

[95] Gibson GM, Leach J, Keen S, Wright AJ, Padgett MJ. Measuring the accuracy of particle position and force in optical tweezers using high-speed video microscopy. Opt Express 2008;16:14561–70. https://doi.org/10.1364/oe.16.014561.
[96] Keen S, Yao A, Leach J, Di Leonardo R, Saunter C, Love G, Cooper J, Padgett M. Multipoint viscosity measurements in microfluidic channels using optical tweezers. Lab Chip 2009;9:2059–62. https://doi.org/10.1039/b900934e.
[97] Hardiman W, Clark M, Friel C, Huett A, Perez-Cota F, Setchfield K, Wright AJ, Tassieri M. Living cells as a biological analog of optical tweezers-a non-invasive microrheology approach. Acta Biomater 2023;166:317–25. https://doi.org/10.1016/j.actbio.2023.04.039.
[98] Favre-Bulle IA, Scott EK. Optical tweezers across scales in cell biology. Trends Cell Biol 2022;32:932–46. https://doi.org/10.1016/j.tcb.2022.05.001.
[99] Roger V, Cottet H, Cipelletti L. A New Robust Estimator of Polydispersity from Dynamic Light Scattering Data. Anal Chem 2016;88:2630–6. https://doi.org/10.1021/acs.analchem.5b03584.
[100] Weatherbee A, Popov I, Vitkin A. Accurate viscosity measurements of flowing aqueous glucose solutions with suspended scatterers using a dynamic light scattering approach with optical coherence tomography. J Biomed Opt 2017:22. https://doi.org/10.1117/1.Jbo.22.8.087003.
[101] Weiss JN, Levy S. Dynamic light scattering spectroscopy of the retina-a non-invasive quantitative technique to objectively document visual improvement following ocular stem cell treatment. Stem Cell Investig 2019;6. https://doi.org/10.21037/sci.2019.03.01. 8-8.
[102] Fröba AP, Leipertz A. Accurate determination of liquid viscosity and surface tension using surface light scattering (SLS):: Toluene under saturation conditions between 260 and 380 K. Int J Thermophys 2003;24:895–921. https://doi.org/10.1023/a:1025097311041.
[103] Adamczyk Z, Cichocki B, Ekiel-Jezewska ML, Slowicka A, Wajnryb E, Wasilewska M. Fibrinogen conformations and charge in electrolyte solutions derived from DLS and dynamic viscosity measurements. J Colloid Interface Sci 2012;385:244–57. https://doi.org/10.1016/j.jcis.2012.07.010.
[104] R.N. Zia, Active and Passive Microrheology: Theory and Simulation, in: S.H. Davis, P. Moin (Eds.) Annu Rev Fluid Mech, Vol 502018, pp. 371–405.
[105] Froeba AP, Leipertz A. Viscosity of diisodecyl phthalate by surface light scattering (SLS). J Chem Eng Data 2007;52:1803–10. https://doi.org/10.1021/je7001623.
[106] Cui J, Bi S, Fröba AP, Wu J. Viscosity and interfacial tension of n-heptane with dissolved carbon dioxide by surface light scattering (SLS). The Journal of Chemical Thermodynamics 2021;152:106266. https://doi.org/10.1016/j.jct.2020.106266.
[107] Koller TM, Prucker T, Cui J, Klein T, Fröba AP. Interfacial tensions and viscosities in multiphase systems by surface light scattering (SLS). J Colloid Interface Sci 2019;538:671–81. https://doi.org/10.1016/j.jcis.2018.11.095.
[108] Klein T, Yan S, Cui J, Magee JW, Kroenlein K, Rausch MH, Koller TM, Fröba AP. Liquid Viscosity and Surface Tension of n-Hexane, n-Octane, n-Decane, and n-Hexadecane up to 573 K by Surface Light Scattering. Journal of Chemical & Engineering Data 2019;64:4116–31. https://doi.org/10.1021/acs.jced.9b00525.
[109] Langevin D. Light scattering by liquid surfaces, new developments. Adv Colloid Interface Sci 2021;289:102368. https://doi.org/10.1016/j.cis.2021.102368.
[110] He F, Becker GW, Litowski JR, Narhi LO, Brems DN, Razinkov VI. High-throughput dynamic light scattering method for measuring viscosity of concentrated protein solutions. Anal Biochem 2010;399:141–3. https://doi.org/10.1016/j.ab.2009.12.003.
[111] Gilroy EL, Hicks MR, Smith DJ, Rodger A. Viscosity of aqueous DNA solutions determined using dynamic light scattering. Analyst 2011;136:4159–63. https://doi.org/10.1039/c1an15475c.
[112] Garting T, Stradner A. Synthesis and application of PEGylated tracer particles for measuring protein solution viscosities using Dynamic Light Scattering-based microrheology. Colloids and Surfaces B: Biointerfaces 2019;181:516–23. https://doi.org/10.1016/j.colsurfb.2019.05.059.
[113] Gazi I, Kim H, Paterson AHJ, Huppertz T. Measuring viscosity of supersaturated lactose solutions using dynamic light scattering. Int Dairy J 2020;102:104596. https://doi.org/10.1016/j.idairyj.2019.104596.
[114] Roriz P, Silva S, Frazão O, Novais S. Optical Fiber Temperature Sensors and Their Biomedical Applications. Sensors (Basel) 2020;20. https://doi.org/10.3390/s20072113.
[115] Leven C, Barrash W. Fiber Optic Pressure Measurements Open Up New Experimental Possibilities in Hydrogeology. Ground Water 2022;60:125–36. https://doi.org/10.1111/gwat.13128.
[116] Yugay V, Mekhtiyev A, Madi P, Neshina Y, Alkina A, Gazizov F, Afanaseva O, Ilyashenko S. Fiber-Optic System for Monitoring Pressure Changes on Mine Support Elements. Sensors (Basel) 2022;22. https://doi.org/10.3390/s22051735.
[117] Maeda M, Kadokura M, Aoki R, Komatsu N, Kawakami M, Koyama Y, Watanabe K, Nishiyama M. A Fiber-Optic Non-Invasive Swallowing Assessment Device Based on a Wearable Pressure Sensor. Sensors (Basel) 2023;23. https://doi.org/10.3390/s23042355.
[118] Feng H, Zhan L, Zhu R, Wang H, Xu F. Endoscopic displacement measurement based on fiber optic bundles. Opt Express 2022;30:14948–57. https://doi.org/10.1364/oe.455510.
[119] Xu B, Yu S, Zhang J. Design Method of Three-Component Optic Fiber Balance Based on Fabry-Perot Displacement Sensor. Sensors (Basel) 2023:23. https://doi.org/10.3390/s23177492.
[120] Mihailovic P, Petricevic S. Fiber Optic Sensors Based on the Faraday Effect. Sensors (Basel) 2021;21. https://doi.org/10.3390/s21196564.
[121] Geng T, Su C, Zhang S, Ma Y. Recent progress in embedded LPFGs. Measurement 2023;222:113686. https://doi.org/10.1016/j.measurement.2023.113686.
[122] Wang JN, Luo CY. Long-period fiber grating sensors for the measurement of liquid level and fluid-flow velocity. Sensors (Basel) 2012;12:4578–93. https://doi.org/10.3390/s120404578.
[123] Wang JN, Tang JL. An optical fiber viscometer based on long-period fiber grating technology and capillary tube mechanism. Sensors (Basel) 2010;10:11174–88. https://doi.org/10.3390/s101211174.
[124] Horan LE, Ruth AA, Gunning FC. Hollow core photonic crystal fiber based viscometer with Raman spectroscopy. J Chem Phys 2012;137:224504. https://doi.org/10.1063/1.4771659.
[125] Ma J, Huang X, Bae H, Zheng Y, Liu C, Zhao M, Yu M. Liquid Viscosity Measurement Using a Vibrating Flexure Hinged Structure and a Fiber-Optic Sensor. IEEE Sens J 2016;16:5249–58. https://doi.org/10.1109/jsen.2016.2562740.
[126] R.D. Pechstedt, Fibre optic pressure and temperature sensor for applications in harsh environments, 5th European Workshop on Optical Fibre Sensors, Krakow, POLAND, 2013.
[127] Qian H, Shao LY, Zhang W, Zhang X, He H, Luo B, Pan W, Zou X, Yan L. Fiber-Optic Viscometer With All-Fiber Acousto-Optic Superlattice Modulated Structure. Journal of Lightwave Technology 2018;36:4123–8. https://doi.org/10.1109/jlt.2018.2859239.
[128] Li D, Wang X, Wang Y, Jiang C, Dong T, Cong Z, Sun J, Chen P. U-shaped optical microfiber-based liquid viscosity measurement. Optical Fiber Technology 2023:81. https://doi.org/10.1016/j.yofte.2023.103502.
[129] Xu C, Zhang Y, Ren M, Liu K, Wu Q, Zhang C, Kong F. Near-infrared dual-response fluorescent probe for detection of N2H4 and intracellular viscosity changes in biological samples and various water samples. Spectrochimica Acta Part A: Molecular and Biomolecular Spectroscopy 2024;314:124180. https://doi.org/10.1016/j.saa.2024.124180.
[130] Zafar R, Arshad Z, Choi NEun, Li X, Hur J. Unravelling the complex adsorption behavior of extracellular polymeric substances onto pristine and UV-aged microplastics using two-dimensional correlation spectroscopy. Chemical Engineering Journal 2023;470:144031. https://doi.org/10.1016/j.cej.2023.144031.
[131] Zhang W, Yuan W, Zhang X, Coronado M. Predicting the dynamic and kinematic viscosities of biodiesel–diesel blends using mid- and near-infrared spectroscopy. Appl Energy 2012;98:122–7. https://doi.org/10.1016/j.apenergy.2012.03.013.
[132] Baptista P, Felizardo P, Menezes JC, Neiva Correia MJ. Multivariate near infrared spectroscopy models for predicting the iodine value, CFPP, kinematic viscosity at 40°C and density at 15°C of biodiesel. Talanta 2008;77:144–51. https://doi.org/10.1016/j.talanta.2008.06.001.
[133] Tat ME, Van Gerpen JH. The kinematic viscosity of biodiesel and its blends with diesel fuel. Journal of the American Oil Chemists Society 1999;76:1511–3. https://doi.org/10.1007/s11746-999-0194-0.
[134] Yuan WQ, Hansen AC, Zhang Q, Tan ZC. Temperature-dependent kinematic viscosity of selected biodiesel fuels and blends with diesel fuel. Journal of the American Oil Chemists Society 2005;82:195–9. https://doi.org/10.1007/s11746-005-5172-6.
[135] Yuan W, Hansen AC, Zhang Q. Predicting the temperature dependent viscosity of biodiesel fuels. Fuel 2009;88:1120–6. https://doi.org/10.1016/j.fuel.2008.11.011.
[136] Fazeli Burestan N, Afkari Sayyah AH, Safi M. Prediction of amylose content, protein content, breakdown, and setback viscosity of Kadusrice and its flour by near-infrared spectroscopy (NIRS) analysis. J Food Process Preserv 2021:45. https://doi.org/10.1111/jfpp.15069.
[137] Cruz C, Arafeh A, Martin PAA, Fonte CP, De Simone A, Oppong FKK, Jeatt W, Rodgers TLL. Assessment of Near-Infrared and Raman Spectroscopy as Analytical Tools to Predict Viscosity of Ice Cream Mixes. Appl Spectrosc 2023;77:764–73. https://doi.org/10.1177/00037028231176824.
[138] Sirisomboon P, Chowbankrang R, Williams P. Evaluation of Apparent Viscosity of Para Rubber Latex by Diffuse Reflection Near-Infrared Spectroscopy. Appl Spectrosc 2012;66:595–9. https://doi.org/10.1366/11-06507.
[139] Zhang W, Yuan W, Zhang X, Coronado M. Predicting the dynamic and kinematic viscosities of biodiesel-diesel blends using mid- and near-infrared spectroscopy. Appl Energy 2012;98:122–7. https://doi.org/10.1016/j.apenergy.2012.03.013.
[140] Haroon K, Arafeh A, Martin P, Rodgers T, Mendoza C, Baker M. Use of inline near-infrared spectroscopy to predict the viscosity of shampoo using multivariate analysis. Int J Cosmet Sci 2019;41:346–56. https://doi.org/10.1111/ics.12536.
[141] Haroon K, Arafeh A, Cunliffe S, Martin P, Rodgers T, Mendoza C, Baker M. Comparison of Individual and Integrated Inline Raman, Near-Infrared, and Mid-Infrared Spectroscopic Models to Predict the Viscosity of Micellar Liquids. Appl Spectrosc 2020;74:819–31. https://doi.org/10.1177/0003702820924043.
[142] Zhang Y, Jiang Q, Wang K, Fang Y, Zhang P, Wei L, Li D, Shu W, Xiao H. Dissecting lysosomal viscosity fluctuations in live cells and liver tissues with an ingenious NIR fluorescent probe. Talanta 2024;272:125825. https://doi.org/10.1016/j.talanta.2024.125825.
[143] Kuimova MK, Yahioglu G, Levitt JA, Suhling K. Molecular rotor measures viscosity of live cells via fluorescence lifetime imaging. J Am Chem Soc 2008;130:6672. https://doi.org/10.1021/ja800570d. -+.
[144] Fu M, Wang K, Ma Q, Zhu J, Bian M, Zhu Q. A novel dual-functional fluorescent probe for imaging viscosity and cysteine in living system. Org Biomol Chem 2022;20:672–7. https://doi.org/10.1039/d1ob02116h.
[145] Liu Y, Ma Y, Gao W, Ma S, Lin W. Construction of a fluorescent probe with large stokes shift and deep red emission for sensing of the viscosity in hyperglycemic mice. Dyes and Pigments 2021:195. https://doi.org/10.1016/j.dyepig.2021.109674.

[146] Ponjavic A, Dench J, Morgan N, Wong JSS. In situ viscosity measurement of confined liquids. RSC Adv 2015;5:99585–93. https://doi.org/10.1039/c5ra19245e.
[147] Parker WC, Chakraborty N, Vrikkis R, Elliott G, Smith S, Moyer PJ. High-resolution intracellular viscosity measurement using time-dependent fluorescence anisotropy. Opt Express 2010;18:16607–17. https://doi.org/10.1364/oe.18.016607.
[148] Arosio P, Hu K, Aprile FA, Muller T, Knowles TP. Microfluidic Diffusion Viscometer for Rapid Analysis of Complex Solutions. Anal Chem 2016;88:3488–93. https://doi.org/10.1021/acs.analchem.5b02930.
[149] Carroll NJ, Jensen KH, Parsa S, Holbrook NM, Weitz DA. Measurement of flow velocity and inference of liquid viscosity in a microfluidic channel by fluorescence photobleaching. Langmuir 2014;30:4868–74. https://doi.org/10.1021/la404891g.
[150] Allmendinger A, Dieu LH, Fischer S, Mueller R, Mahler HC, Huwyler J. High-throughput viscosity measurement using capillary electrophoresis instrumentation and its application to protein formulation. J Pharm Biomed Anal 2014;99:51–8. https://doi.org/10.1016/j.jpba.2014.07.005.
[151] Del Giudice F. A Review of Microfluidic Devices for Rheological Characterisation. Micromachines (Basel) 2022;13. https://doi.org/10.3390/mi13020167.
[152] Karamzadeh V, Sohrabi-Kashani A, Shen M, Juncker D. Digital Manufacturing of Functional Ready-to-Use Microfluidic Systems. Adv Mater 2023;35:e2303867. https://doi.org/10.1002/adma.202303867.
[153] P. Jones, O.M. Marago, G. Volpe, Optical Tweezers: Principles & Applications, 2015.
[154] Blázquez-Castro A. Optical Tweezers: Phototoxicity and Thermal Stress in Cells and Biomolecules. Micromachines (Basel) 2019:10. https://doi.org/10.3390/mi10080507.
[155] Halma MTJ, Tuszynski JA, Wuite GJL. Optical tweezers for drug discovery. Drug Discov Today 2023;28:103443. https://doi.org/10.1016/j.drudis.2022.103443.
[156] Koller TM, Kerscher M, Fröba AP. Accurate determination of viscosity and surface tension by surface light scattering in the presence of a contribution from the rotational flow in the bulk of the fluid. J Colloid Interface Sci 2022;626:899–915. https://doi.org/10.1016/j.jcis.2022.06.129.
[157] Zhai Z, Paap U, Gezmis A, Maier F, Steinrück HP, Koller TM. Surface tension and viscosity of binary ionic liquid mixtures from high vacuum up to pressures of 10 MPa. J Mol Liq 2023;386:122388. https://doi.org/10.1016/j.molliq.2023.122388.
[158] Cadogan SP, Hahn CJ, Rausch MH, Fröba AP. Study on the applicability of dynamic light scattering (DLS) to microemulsions including supercritical carbon dioxide-swollen micelles. J Colloid Interface Sci 2017;499:202–8. https://doi.org/10.1016/j.jcis.2017.03.111.
[159] R.D. Pechstedt, Fibre optic pressure and temperature sensor for applications in harsh environments, Proc.SPIE2013, pp. 879405.
[160] Su WH, He HJ, Sun DW. Non-Destructive and rapid evaluation of staple foods quality by using spectroscopic techniques: A review. Crit Rev Food Sci Nutr 2017;57:1039–51. https://doi.org/10.1080/10408398.2015.1082966.
[161] Webb JK, Lee CC, Carswell RF, Milaković D. Getting the model right: an information criterion for spectroscopy. Mon Not R Astron Soc 2020;501:2268–78. https://doi.org/10.1093/mnras/staa3551.
[162] Xue X, Sun H, Yang M, Liu X, Hu HY, Deng Y, Wang X. Advances in the Application of Artificial Intelligence-Based Spectral Data Interpretation: A Perspective. Anal Chem 2023;95:13733–45. https://doi.org/10.1021/acs.analchem.3c02540.
[163] Yeh HW, Ai HW. Development and Applications of Bioluminescent and Chemiluminescent Reporters and Biosensors. Annu Rev Anal Chem (Palo Alto Calif) 2019;12:129–50. https://doi.org/10.1146/annurev-anchem-061318-115027.
[164] Fang PW, Lin YC, Fan SY, Panja A, Xu SQ, Lee SH, Tan KT. Protein-Labeling Fluorescent Probe for Folate Receptor α. Anal Chem 2023;95:11535–41. https://doi.org/10.1021/acs.analchem.3c02215.
[165] Lin M, Liu S. Naphthalimide-Based Fluorescent Probe for Profiling of Aldehydes during Oxidation of Unsaturated Lipids. J Agric Food Chem 2022;70:14304–11. https://doi.org/10.1021/acs.jafc.2c05659.
[166] Lin X, Li Z, Bu D, Liu W, Li Z, Wei R, Yu M. Multiple organelle-targeted near-infrared fluorescent probes toward pH and viscosity. Spectrochim Acta A Mol Biomol Spectrosc 2022;283:121665. https://doi.org/10.1016/j.saa.2022.121665.
[167] Efimov IR, Nikolski VP, Salama G. Optical imaging of the heart. Circ Res 2004;95:21–33. https://doi.org/10.1161/01.RES.0000130529.18016.35.
[168] Del Giudice F, Sathish S, D'Avino G, Shen AQ. "From the Edge to the Center": Viscoelastic Migration of Particles and Cells in a Strongly Shear-Thinning Liquid Flowing in a Microchannel. Anal Chem 2017;89:13146–59. https://doi.org/10.1021/acs.analchem.7b02450.
[169] Kornaeva EP, Stebakov IN, Kornaev AV, Dremin VV, Popov SG, Vinokurov AY. A method to measure non-Newtonian fluids viscosity using inertial viscometer with a computer vision system. Int J Mech Sci 2023;242:107967. https://doi.org/10.1016/j.ijmecsci.2022.107967.
[170] Stender AS, Marchuk K, Liu C, Sander S, Meyer MW, Smith EA, Neupane B, Wang G, Li J, Cheng JX, Huang B, Fang N. Single cell optical imaging and spectroscopy. Chem Rev 2013;113:2469–527. https://doi.org/10.1021/cr300336e.
[171] Omar AA, Farag MM, Alhamad RA. Ieee, Artifical Intelligence: New Paradigm in Deep Space Exploration. In: 14th International Conference on Developments in eSystems Engineering (DeSE). Univ Sharjah; 2021. p. 438–42.
[172] Integrated Imaging and Vision Techniques for Industrial Inspection: Advances and Applications, in: Z. Liu, H. Ukida, P. Ramuhalli, K. Niel (Eds.) Integrated Imaging and Vision Techniques for Industrial Inspection: Advances and Applications 2015, pp. 1–541.
[173] Abu Ebayyeh AARM, Mousavi A. A Review and Analysis of Automatic Optical Inspection and Quality Monitoring Methods in Electronics Industry. Ieee Access 2020;8:183192–271. https://doi.org/10.1109/access.2020.3029127.
[174] Battat S, Weitz DA, Whitesides GM. An outlook on microfluidics: the promise and the challenge. Lab Chip 2022;22:530–6. https://doi.org/10.1039/d1lc00731a.
[175] Wang W, Xia L, Xiao X, Li G. Recent Progress on Microfluidics Integrated with Fiber-Optic Sensors for On-Site Detection. Sensors 2024:24. https://doi.org/10.3390/s24072067.
[176] François Y, Zhang K, Varenne A, Gareil P. New integrated measurement protocol using capillary electrophoresis instrumentation for the determination of viscosity, conductivity and absorbance of ionic liquid–molecular solvent mixtures. Anal Chim Acta 2006;562:164–70. https://doi.org/10.1016/j.aca.2006.01.036.
[177] Lipus MP, Kranz S, Reinsch T, Cunow C, Henninges J, Reich M. Distributed viscosity and flow velocity measurements using a fiber-optic shear stress sensor. Sensors and Actuators A: Physical 2022;345:113760. https://doi.org/10.1016/j.sna.2022.113760.
[178] Zhang X, Zhao G, Yin J, Ma S. Experimental investigation of saturated liquid kinematic viscosity and surface tension of two isomeric refrigerants trans-1,1,1,4,4,4-hexafluoro-butene (R1336mzz(E)) and cis-1,1,1,4,4,4-hexafluoro-butene (R1336mzz(Z)) by surface light scattering. Fluid Phase Equilib 2022;559:113468. https://doi.org/10.1016/j.fluid.2022.113468.